TSEM Texas Society for Electron Microscopy e⁻ NEWSLETTER

Spring, 1977

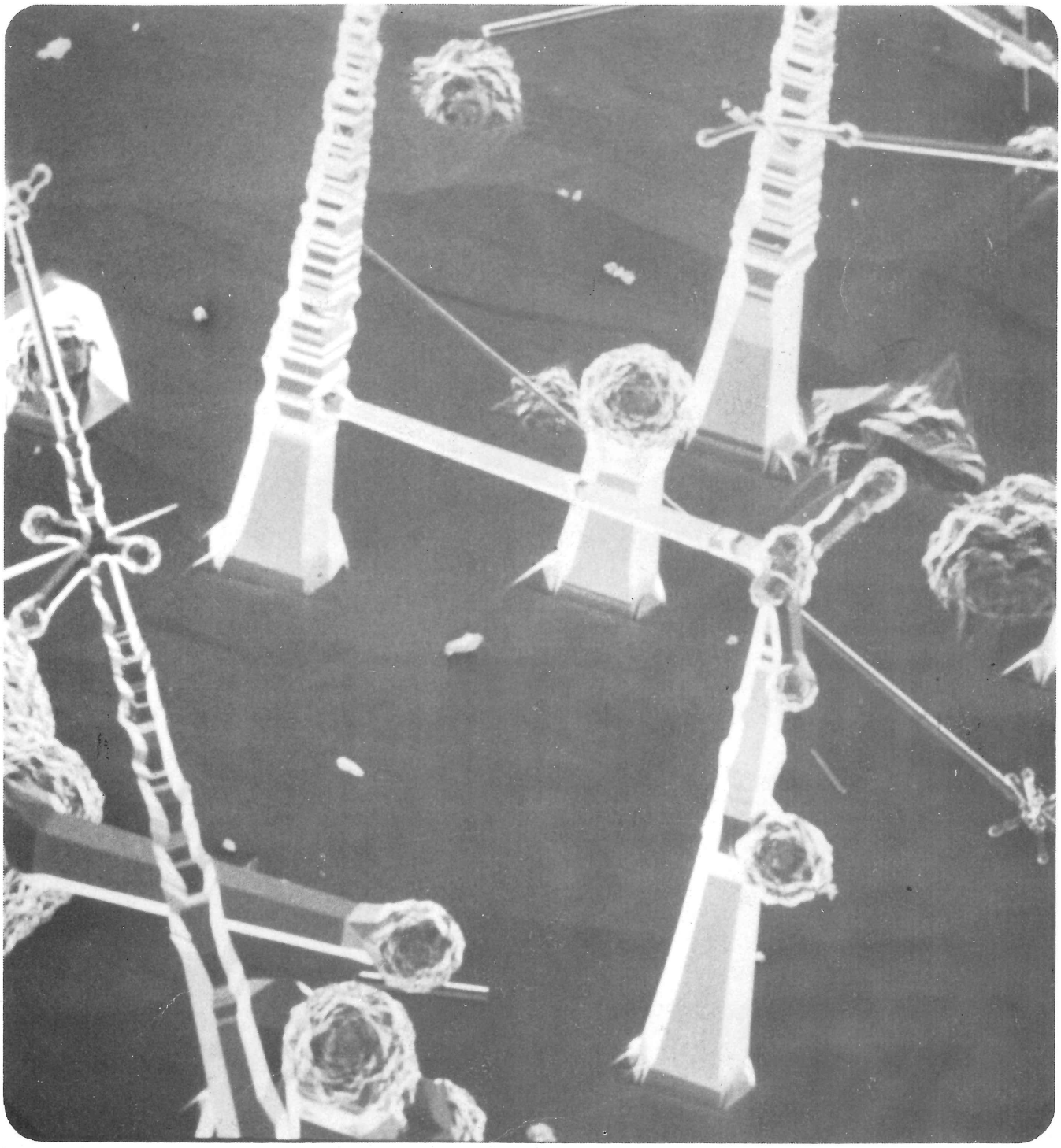

The very latest in research-quality SEM's

The ISI-60 (left) and the SUPER III-A.

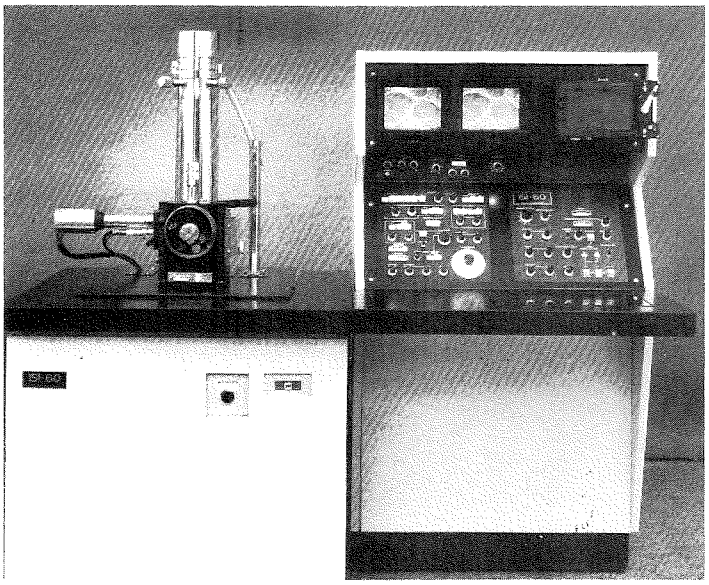

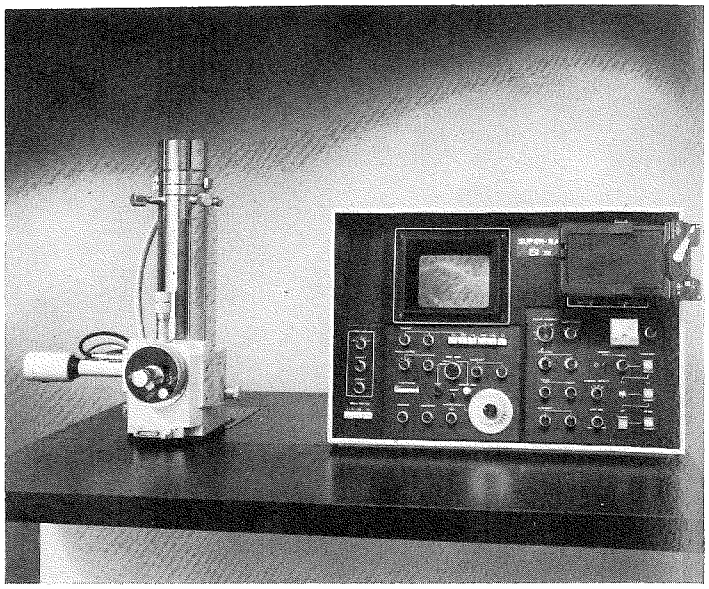

More SEM's to choose from

ISI's policy is to offer the scientific community scanning electron microscopes that satisfy both performance and budget requirements. On the front page of this flyer, you have seen our top-of-the-line SEM'S, the ISI-60 and the SUPER III-A. For those who are budget-limited, ISI also offers three additional fine-performing SEM's. The SUPER II, with a guaranteed resolution of 70 Angstroms, satisfies many requirements and is priced at less than $20,000. For educators, production and quality control applications, the Model 7 and the TV MINI-SEM® provide from 100 to 500 Angstroms resolution and are priced from $12,000 to $18,000 — the lowest priced high performance SEM's in the world.

For complete details on any of these fine instruments, contact your local ISI office shown below.

ISI Connecticut
795 North Mountain Road
Newington, CT 06111
(203) 246-5639

ISI Southeast
1840-18 Jerry Way
Norcross, GA 30093
(404) 233-7218

ISI Southwest
6655 Hillcroft, Suite 100
Houston, TX 77081
(713) 777-0321

ISI Chicago
799 Roosevelt Road, Building 3,
Suite 11
Glen Ellyn, IL 60137
(312) 858-1244

CAL-SEM Associates
1926 Pacific Coast Highway,
Suite 109-B
Redondo Beach, CA 90277
(213) 375-5422

ISI West Coast
1400 Stierlin Road
Mountain View, CA 94043
(415) 965-8600

Allan Crawford Associates
1299 Richmond Road
Ottawa, Ontario K2B 7Y4
(613) 829-9651

INTERNATIONAL SCIENTIFIC INSTRUMENTS, INC.
1400 Stierlin Road
Mountain View, CA 94043
Phone (415) 965-8600

ISI International Scientific Instruments, Inc.

Headquarters: 1400 Stierlin Road • Mountain View, CA 94043 • Phone (415) 965-8600
Sales and service around the world

Contents

Volume 8, Number 3
Spring, 1977

Texas Society for Electron Microscopy
"For the purpose of dissemination of research with the electron microscope"

President's Message

I want to take this opportunity to thank the membership of TSEM for its support during this past year. The fall meeting at Scott & White was a success and the society would like to thank the hospital staff, administration, and the Broders foundation for their support. The winter symposium was most successful and represented the first time the Texas, Louisiana and Southeastern states held a joint symposium. The Austin meeting will have a special session devoted to the material sciences and feature nationally known guest speakers. The fall meeting will be held in Arlington, Texas in conjunction with the University of Texas and the program will center around a two day workshop on stereology. Student travel scholarship support has been extended to include all three yearly meetings.

This society owes its existence and maintenance to the officer corp and appointed personnel who contribute their time and effort in support of TSEM. I want to thank my executive committee and appointed personnel for their support. This is one of the most active EM societies in the United States and it will take your continued effort to maintain its momentum. I am proud that I had the opportunity to serve as an officer in the Texas Society for the Electron Microscopy.

E. LAURENCE THURSTON
President

March 25, 1977

TEXAS SOCIETY FOR ELECTRON MICROSCOPY
c/o Mr. Robert A. Turner
TSEM Newsletter Editor
Scott & White Clinic
Temple, Texas 76501

Dear TSEM Colleagues:

The 6th Annual Joint Symposium of the Texas & Louisiana Societies for Electron Microscopy and The Annual Meeting of the Southeast Society for Electron Microscopy is history, and by all standards, this joint conference must be considered an outstanding scientific achievement by our three local societies. The interest and participation by TSEM, as always, was of paramount and vital importance to the Symposium. In addition, the presence of SEEMS and tremendous response by our corporate exhibitors added an "icing on the cake" aspect which certainly enhanced the proven success and value of this Symposium. The Executive Council and general membership of LSEM are proud and most gratified for hosting this important event. We take this opportunity to thank our many visitors who, in essence, are the most important ingredient of any scientific endeavour.

We wish you well with the 7th Joint TSEM/LSEM Symposium. Please call on us if we can be of service.

Respectfully yours,

Joe A. Mascorro
Local Arrangements Chairman
6th Joint TSEM/LSEM Symposium and
The Annual SEEMS Meeting.

Editor's Comments

As Editor of your TSEM Newsletter, I have been asked and told to write these comments.

At first thought, I was baffled as to what subject to write about. Actually, I had several choices of subjects from which to choose, such as the recent LSEM, TSEM, SEEM symposium held in oyster-laden New Orleans; how great our local society has become in twelve short years; how great and beautiful our corporate members have been to TSEM, especially local "reps"; future TSEM meetings or just a plain BS session with my friends throughout this great lone star state.

After much thought, consideration and dilemma, I have decided to elaborate on none of the above subjects.

For the sake of our prestigious out-going president, Dr. E. Laurence Thurston, I am not going to stand on my "soapbox" and tell you how great our society is, (it speaks for itself) but instead I am going to express my personal feelings about a recent "transfer" of one of our greatest and most faithful members, (C.) Ward Kischer. Ward, besides being a long time member of our society, has made enormous and countless contributions to our society. Not only is a past president (a darn good one too!), but was the second editor of this grand and glorious newsletter. Ward is of course by profession a Ph.D. anatomist, but in my opinion should have been a journalist for the Washington Post or New York Times. He is and always will be a natural journalist, another Ben Franklin. We have lost Ward to a group of researchers and scientists in Tucson, Arizona and unfortunately he won't be attending very many future TSEM meetings. I think and personally feel we all will miss Ward in the crowds, paper sessions and especially at our colorful socials. It has been my personal pleasure to have known this great guy for over ten years and he will always be welcomed back to Texas and future TSEM meetings. GOOD LUCK, WARD!

If I sound too philosophic, it's because I am composing this at the local bowling alley while my wife is competing in her womans' bowling league.

Just in closing, please keep the articles, micrographs, area news, and especially the advertisements — money — coming, because after all it's you, the members, that make this newsletter what it is today.

Robert A. Turner
TSEM Newsletter Editor

TSEM FINANCIAL REPORT

Period Ending March 25, 1977

Total Assets December 8, 1976		$ 7,490.84
Certificate of Deposit (University Bank No. 4470)		1,197.13
Certificate of Deposit (Fannin Bank No. 17864)		1,000.00
Savings Account (Fannin Bank No. 12-0900043)		3,172.30
Balance in Checking Account December 8, 1976		$ 2,121.41
RECEIPTS		
EMSA (Winter Meeting 1978)	$ 500.00	
Corporate Dues	300.00	
Member Dues	306.50	
Scott and White Hospital (Fall Meeting)	160.38	
Total Income	$ 1,266.88	$ 1,266.88
		$ 3,388.29
DISBURSEMENTS		
Advance for Spring Meeting, 1977 (Mitchell)	$ 150.00	
Secretarial Expenses (Hillman)	500.00	
Newsletter Expense (Turner)	500.00	
Travel to New Orleans	118.00	
Total Expenses	$ 1,268.00	$ 1,268.00
Balance in Checking Account March 25, 1977		$ 2,120.29
SAVINGS ACCOUNTS		
Certificate of Deposit (University Bank No. 4470)		$ 1,215.22
Certificate of Deposit (Fannin Bank No. 17864)		1,000.00
Savings Account (Fannin Bank No. 12-0900043)		3,230.89
TOTAL ASSETS March 25, 1977		**$ 7,566.40**

Calibration and Test Specimens for SEM

Each specimen securely affixed to an aluminum stud. **Please specify stud you need.**

Cat. No. 31500
Low Magnification Calibration Specimen
Precision copper screening, 400 mesh, is affixed to the center of a specimen stud. This screening calibrates specimens at magnifications from 50X to 500X.

On the same stud, 1000 mesh copper screening is positioned to one side. This screening calibrates specimens at magnifications from 500X to 1000X.

Both screenings are exceptionally uniform in all dimensions

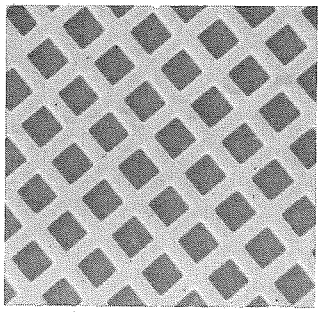

100x

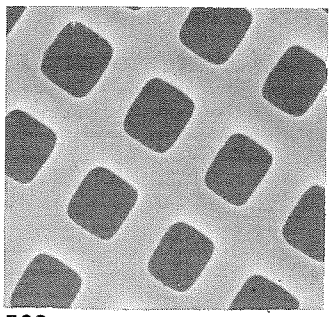

500x

Cat No. 31550
Grating – 15,240 lines per inch
Made specifically for use in scanning electron microscopes. This replica is taken from a ruled diffraction grating with 15,240 lines per inch.

Very useful for magnification determination in the range 1000X to 15,000X.

Measurement chart and instructions included.

Cat. No. 31650 – Grating – "Waffle" Type – A dependably accurate, easy to use specimen, specifically made for use in scanning electron microscopy. The original replica is taken from a diffraction grating with two sets of lines ruled at right angles to each other.

Very useful over a magnification range of 10,000X to 50,000X. It is also used for detection and measurement of lens distortion and determination of the degree of fore-shortening in an image, as a function of specimen tilt.
Measurement chart and instructions included

Cat. No. 31700 – Composite Magnification Test Specimen – Composed of three magnification specimens attached firmly to a scanning microscope specimen stud. One specimen is 400 mesh copper screening for low magnification work. The middle specimen is a 1500 mesh silver screening for the middle magnification range. The third specimen is a 15,240 lines per inch grating for the medium high magnification range.

This composite specimen is both a time and space saver.
Measurement charts and instructions for use included

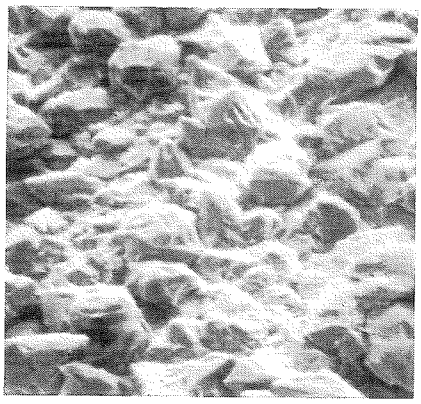

Surface detail of Gold Mesh Bar. 2000X

Cat. No. 62120
Image Quality Checker

– A specimen of 200 mesh gold screening is firmly affixed to an SEM stud. This provides a quick method of determining image quality. Good surface detail discernible at reasonably high magnification. Will not oxidize. Please state stud you need.

For further information, fill out coupon at right and mail to:

Ladd Research Industries, inc.

P.O. Box 901, Burlington, Vermont 05402
Or telephone us at **802-658-4961**

Gentlemen: Please send me the following:

☐ FREE Ladd Catalog of Scientific Information

☐ Information on Catalog No. _____

☐ Name and Address of Local Distributor

Name _____

Company or School _____

Address _____

City _____ State _____ Zip _____

The Characterization Of Solid Surfaces

By Graydon B. Larrabee
Materials Characterization Laboratory
Texas Instruments Incorporated
P.O. Box 5936, MS 147, Dallas, Texas 75222

KEYWORDS
Surface Analysis, Topography, Defects, Electron Beam Techniques, Ion Beam Techniques, Photon Techniques.

Abstract

The purpose of this tutorial is to review and compare surfaces characterization techniques. The techniques have been broken into two broad categories, one group covering microtopography and defects and the other covering chemical characterization of surfaces. An effort has been made to choose the most commonly used techniques with consideration in the choice given to maturity and commercial availability of each technique.

In surface microtopography the role of optical microscopy, scanning electron microscopy, profilometry and optical interferometry are discussed. Each technique has a specific strength in characterization of a surface depending on whether information is required in the lateral, x-y, or vertical, z, direction. Microdefects often can be characterized using electron diffraction, optical microscopy or x-ray diffraction.

The surface characterization techniques chosen for chemical characterization are divided into three categories based on the excitation process; electrons, ions, and photons. The electron beam techniques, as a group, have the best spatial resolution and imaging capabilities. The ion beam techniques all provide good in-depth analytical capability. The mutual exclusiveness of analyzing trace amounts of elements and analyzing elements in extremely small (microanalysis) volumes is clearly demonstrated for all techniques. The effects on characterization results of changing instrument operating conditions (parameters) are given for both electron and ion beam techniques.

Introduction

The characterization of a solid surface involves substantially more than an image of the surface topography or a chemical analysis of the outer monolayer of atoms on that surface. Characterization must be a coordinated description of the surface composition and structure (including defects) that is sufficient to study the surface properties, or use, and suffices for reproduction of that surface. This description of surface characterization is an adaptation of the definition of materials characterization adopted by the Materials Advisory Board.[1] Initially, it may appear that surface characterization of this quality and detail may not be attainable. However, as was pointed out in an earlier publication,[2] there has been a dramatic consolidation of many analytical techniques into characterization systems. Incorporation of secondary electron, backscattered electron, x-ray, Auger electron, transmitted electron and diffracted electron detectors in systems is now common practice. As a result, it is frequently possible to obtain high resolution topographic (x-y) and compositional images of a surface in one analytical instrument. In-depth analysis (z-direction) with 2 nm resolution is readily attainable when a sputter gun is incorporated as part of the system. Electron diffraction data can yield both crystallographic information, e.g. α and β forms of SiO_2, and chemical compound identification from d spacing of diffracted electrons.

As can be seen, complete characterization of a surface is far more feasible today than it was a year or two ago. The problem of every analyst working in this field is to understand the capabilities and limitations of each of a myriad of characterization tools. The reader is referred to the excellent reviews of Evans,[3,4] Mayer[5] and Wittry.[6] A list of the surface characterization techniques in use today is shown in Table I. This list, which includes the most commonly associated acronyms, is broken down into the categories of electrons, ions and photons. This breakdown is difficult to define unambiguously, but in this case, an effort has been made to assign the techniques to a

particular mode of excitation. There are obvious exceptions, but for the purposes of this review these categories will suffice.

TABLE I
SURFACE CHARACTERIZATION TECHNIQUES

Technique	Acronym
ELECTRONS	
Appearance Potential Spectroscopy	APS
Auger Electron Spectroscopy	AES
Electron Microprobe	EMP
Electron Microscopy/Diffraction	TEM/D
Low Energy Electron Diffraction	LEED
Scanning Auger Microprobe	SAM
Scanning Electron Microscopy	SEM
SEM with Si Solid State Detector	SEM-Si(Li)
Scanning Transmission Electron Microscopy	STEM
IONS	
Field Ion Microscopy	FIM
Glow Discharge Mass Spectroscopy	GDMS
Glow Discharge Optical Spectroscopy	GDOS
Ion Backscattering Spectroscopy	BS
Ion Induced X-Ray Fluorescence	IIXF
Ion Luminescence Spectroscopy	SCANIIR
Ion Microprobe Mass Analysis	IMMA
Ion Scattering Spectroscopy	ISS
Particle Induced Nuclear Reactions	PAA, NAA
Secondary Ion Mass Spectroscopy	SIMS
PHOTONS	
Ellipsometry	ELL
Optical Interferometry	OI
Optical Microscopy	OM
Optical Spectroscopy, (IR, emission)	OS
Photoelectron Spectroscopy (X-Ray, UV)	ESCA, PES
X-Ray Diffraction	XRD
X-Ray Fluorescence	XRF

A more logical correlation of techniques by exciter and emission of electrons, ions and photons is shown in Table II. It is interesting to notice that while all forms of excitation result in the emission of x-rays only the interaction of ions with a surface results in the emission of ions from a surface. In retrospect this is not unexpected because of the large amounts of energy required to break chemical bonds and to move the ions away from the surface. One area of this table that does not have a technique listed is excitation with ions with the detection of electrons, particularly Auger and secondary electrons. The addition of these detectors to existing ion probes could result in a very comprehensive analytical technique.

In a survey of surface characterization techniques there is always an acrimonious discussion of "what is a surface." Certainly, each analytical technique will result in a different surface description. For example, Auger spectroscopy analyzes 0.5 to 2.0 nm into a surface while x-ray emitting techniques (EMP, XRF) analyze 1 to 25 μm into the surface. The "correct" answer always involves a number of analytical techniques and all contribute to what was described earlier as a "coordinated description of the surface." The specific needs of the analysis will help define the surface, e.g., an inclusion, microprecipitate, film, etc. As will be discussed later in this paper there is a significant difference between microanalysis and trace analysis. Both contribute to a description of the surface but neither is correct nor incorrect when taken alone. Similarly, a topographic analysis in the x-y plane is as valuable as the in-depth or z-direction analysis, i.e., both contribute to a coordinated description of the surface.

In order to limit the scope of this discussion, it is necessary to select the more widely applicable surface characterization techniques to be covered in this review. The current state-of-the-art, commercial availability, maturity and applicability are summarized in Table III. There is, unavoidably, some bias introduced in a subjective evaluation of this type. The last column, labeled "overall" is the epitome of subjectivity on the part of the author. One technique which appears to be an obvious omission is the exciting new analytical technique STEM —scanning transmission electron microscopy. STEM instruments include SEM, x-ray, electron diffraction, backscattered electron, energy loss analysis as well as a transmitted electron detectors. The first four detectors in this list will be covered under more specific instrumentation, while the last two are not for surface analysis. All techniques classified as immature were excluded because they were felt to be in an evolutionary phase of development.

The techniques to be covered in this paper have been broken into two main categories depending on the ultimate goal of the analysis. The first group will cover surface topography and surface defects while the second group will cover chemical composition and contamination of surfaces.

Surface Topography and Defects

In surface characterization, the first parameter that is examined is the physical microtopography. In virtually every application, e.g., surface adhesion, catalysis, semiconductor processing, wear, friction, reflectivity, etc., there is an immediate need to understand the relief of the surface in the x, y, and z direction. The presence of microdefects such as precipitates or inclusions can play an important role in the ultimate properties of the surface.

TABLE II
SURVEY OF TECHNIQUES FOR THE CHARACTERIZATION OF SURFACES

EXCITATION / EMISSION	ELECTRONS	IONS	PHOTONS
ELECTRONS	AES EM LEED SAM SEM STEM		ESCA PES
IONS		FIM GDMS BS IMMA ISS SIMS	
PHOTONS	APS EMP SEM-Si(Li)	GDOS IIXF NAA SCANIIR	ELL OI OM OS XRD XRF XRT

Topography. A list of the most commonly used surface topography and defect characterization techniques is shown in Table IV. An effort has been made to provide the expected best resolution for each technique in the vertical or z-direction and the horizontal or x-y directions. As can be seen, there are substantial differences in ultimate resolution between techniques but also notice there are substantial differences in costs of the equipment. Optical microscopy has always been the most widely applied and least expensive characterization tool for the analyst. There are very few laboratories, where surface characterization is performed, that do not have a number of types of optical microscopes for the first examination of the surface. Generally, decisions on the next step in surface characterization are made from this first optical examination.

There are some interesting countercurrents underway in the scientific community which will narrow the role of optical microscopy. The costs of good optical microscopes have continued to increase along with inflation. On the other hand, scanning electron microscope prices have continued to decline to the point where the top-of-the-line optical microscopes and "inexpensive" SEM instruments are equal in price. At this price level, the SEM has x-y resolution in the 25 nm range compared to 200 nm for the optical microscope and the depth of field in the SEM is 100 to 300 times better. As a result, many laboratories are acquiring SEM instruments rather than optical microscopes. It appears that the trend will continue over the next decade.

TABLE III
STATE-OF-THE-ART, APPLICABILITY, AVAILABILITY

Technique	Maturity	Applicability	Available	Reviewed
ELECTRONS				
APS	Immature	Limited	No	No
AES	Mature	Wide	Yes	Yes
EMP	Mature	Wide	Yes	Yes
TEM/D	Mature	Limited	Yes	No
LEED	Mature	Limited	Yes	No
SAM	New	Developing	Yes	Yes
SEM	Mature	Wide	Yes	Yes
SEM-Si(Li)	Mature	Wide	Yes	Yes
STEM	New	Developing	Yes	Yes
IONS				
FIM	Mature	Limited	No	No
GDMS	Immature	Unknown	No	No
GDOS	Immature	Unknown	Yes	No
BS	Mature	Limited	Yes	Yes
IIXF	Developing	Developing	No	Yes
SCANIIR	Immature	Unknown	No	No
IMMA	Mature	Wide	Yes	Yes
ISS	Mature	Developing	Yes	Yes
PAA, NAA	Mature	Limited	No	No
SIMS	Mature	Wide	Yes	Yes
PHOTONS				
ELL	Mature	Limited	Yes	No
OI	Mature	Limited	Yes	No
OM	Mature	Limited	Yes	No
OS	Mature	Limited	Yes	No
ESCA	Mature	Wide	Yes	Yes
XRD	Mature	Limited	Yes	No
XRF	Mature	Wide	Yes	Yes

The role of the profilometer will narrow in the same way as the optical microscope due to cost pressures on these stylus instruments from SEM manufacturers. There are many applications where stylus instruments serve a unique function that is not easily duplicated by other surface characterization techniques. The very nature of the profilometer dictates that only one cross section of a surface is measure at one time. In quality control of surfaces in metal finishing, optical polishing, etc., this one cross section is the ideal tool to provide a permanent trace which is readily quantified through satistical processing of the line profiles. Stylus techniques can handle very large specimens that cannot be characterized by other techniques. Whole sureaces can be mapped by making repeated side by side line profiles and contour maps of the z surface generated through computer analysis. The SEM undoubtedly provides a better 3-dimensional image of the surface but profilometry can quantitate surface topography. Profilometry has better z resolution and about equal horizontal resolution as optical microscopy.

TABLE IV
SURFACE TOPOGRAPHY AND DEFECT CHARACTERIZATION*

	Z Res.	X-Y Res.	Mag. Range X,	Cost $K
TOPOGRAPHY				
Optical Interferometry	2.5 nm	2.0 μm	1000-100,000	1-7
Optical Microscopy	1.0 μm	0.2 μm	1-1000	1-30
Profilometry	10 nm	0.1 μm	1-20,000	10-15
SEM	50 nm	3.0 nm	10-50,000	10-50
Electron Microscopy	2.0 nm	2.0 nm	1000-100,000	30-100
DEFECTS				
Electron Diffraction	50 nm	50 nm		30-100
Optical Microscopy	1 μm	1 μm	1-200	1-30
X-Ray Diffraction	10 μm	1 μm	1-1000	10-30

* Non-chemical information

Optical interferometry is essentially an extension of optical microscopy. In this characterization one does not see what is classically thought of as a 2-dimensional image of the surface but rather lines of interference. Optical microscopy can resolve detail as small as half a light wave ($\lambda/2$). Multiple beam interferometry is a sensitive surface characterization technique for measuring surface topography in the z direction. It gives limited information in the x-y plane, but does show how z changes with x-y position.

Electron microscopy is frequently used to examine surface topography through replication. Replication when combined with heavy metal (usually platinum-carbon) shadowing allows very good resolution, $\simeq$ 2 nm, of vertical features. This resolution is generally controlled by the granularity of the shadowing agent. Point to point resolution in the x-y plane is in the order of 2 nm. It is interesting to note that the new SEM instruments equipped with field emission electron guns have resolutions in the 2 to 3 nm range while still retaining the excelling depth of field associated with this technique. Vertical resolution of the SEM depends upon the ability to tilt the sample to very high angles, $> 85°$, to image the vertical plane. Resolutions in the order of 50 nm are attainable but resolution is highly sample dependent.

Defects. As was mentioned earlier, all surfaces have

microdefects such as precipitates and inclusions which can be frequently identified by optical microscopy, electron diffraction or x-ray diffraction. In this section chemical analysis of the defect will not be discussed. Chemical composition of defects will be described in considerable detail in the section on chemical surface composition.

An experienced optical microscopist can identify many defects from shape, color, luster, etc. Polarized light is frequently employed or combined with chemical stains or decoration to aid in this identifucation. The side of the defect usually must be larger than 50 μm, however, the defect need not be crystalline as is the case for electron and x-ray diffraction techniques. This type of surface analysis is, of course, qualitative but is also a valuable tool when combined with chemical compositional microanalysis techniques.

A typical electron-beam diameter used in electron diffraction is 10 μm. Since the surface and electron beams are at very low grazing angles, $\simeq 0.5°$, the length of a flat surface irradiated is near 1 mm. If the defect is crystalline or polycrystalline a diffraction pattern will be obtained and an identification is possible from measured d spacings. In ideal cases, the beam diameter can be much smaller, $\simeq$ 50 nm, and diffraction patterns can be obtained from defects in the 50 nm range. If the defect is amorphous then electron diffraction is not possible and this case often occurs when precipitates, e.g., SiO_2, SiC, in matrices such as silicon or metals.

The use of x-ray diffraction methods to examine a particular microdefect on a surface is limited by the inability to focus or collimate x-rays to obtain microbeams. The large penetrating power of x-rays means that analyses are made 5 to 10 μm into the sample. Standard Laue techniques can be used to obtain particle size, non-uniform strain, faulting and lattice parameters in ideal surfaces to a depth of 1 μm. X-ray topography is used to map the distribution of individual dislocations in near perfect single crystal surfaces ($> 10^5$ dislocations/cm^2). This technique measures strain in a single crystal and therefore defects such as microprecipitates are seen indirectly. A resolution if 1 μm is possible in ideal cases and this is limited by the photographic emulsion used to record the x-ray topographic image.

Chemical Surface Composition and Contamination

The chemical composition of a surface is not intuitively clear unless some guidelines or definitions are agreed upon. For example, virtually all metals have a native oxide on the surface which can vary in thickness from 1 to 10 nm. The surface of these metals that is most commonly encountered and the surface that controls the chemical and mechanical properties is the oxide, not the metal. However, where a surface compositional analysis is performed on a metal, alloy, or evaporated film, this outer native oxide is either not considered or is physically removed by ion etching, cleaving in vacuum, mechanical or chemical polishing. As will be described later, techniques that do not employ ion sputtering such as x-ray fluorescence and electron microprobe analyze from 1 to 25 μm into the surface and do not "see" the thin native oxide. Therefore, chemical surface composition may look considerably different depending on the characterization technique employed. When the analytical capabilities of the characterization technique are taken into consideration, the chemical surface composition is understandable and becomes part of the coordinated description of the surface referred to in the introduction.

Surface contamination is that part of the surface which lies on or in the native oxide or native surface of the material being analyzed. Normally this consists of absorbed or adsorbed gases, organic materials, water, inorganic ions and electrochemically deposited metals from trace impurities in chemical reagents. These surface contamination layers are generally very then, 0.5 to 10 nm in thickness, but have chemical compositions which have high elemental concentrations, $> 10\%$. Thus, surface analysis of contaminated surfaces does not involve trace analysis but rather the microchemical analysis of very thin layers. This still requires very high analytical sensitivity since a 1 nm thick layer weighs $\sim 2 \times 10^{-7}$ g/cm^2 and contains $\sim 5 \times 10^{15}$ atoms/cm^2. Analysis for chemical compositions in the 10% range is a challening task.

It is importent to define the difference between trace analysis and microanalysis in surface characterization because some techniques excel in one category or the other. For the purpose of this review, trace analysis will be defined as the determination of elemental concentrations of less than 1000 ppma without regard to sample size. Microanalysis is the characterization of microsamples or microvolumes where the diameter of the area of analysis is less than 10 μm. The term microanalysis defines size without regard to elemental concentration. As will be shown later in this review, trace analysis and microanalysis are not mutually compatible. In surface characterization there is always a trade off of one with the other.

This interchange is immediately apparent in both electron beam and ion beam techniques. Figure 1 shows the relationship between beam diameter and beam current for ions and electrons in microprobe instruments. The elemental sensitivity for all ion and electron beam techniques is directly proportional to the beam current. In order to perform microanalysis of areas with diameters in the 100 nm range the beam currents and elemental sensitivity decrease by factors of 1000 to 10,000 compared to 10 μm diameter spots. Table V shows the minimum diameter, the range and optimum diameter for the surface analysis techniques chosen for this review. There is a wide range, however, the electron beam techniques and one ion beam technique (IMMA) are best adapted to microanalysis. Another way of summarizing the diameter of analysis area by technique is shown in Figure 2. Some examples of typical sample diameters is shown on the left side of the chart with range of analytical diameters on the right. Notice the wide analytical range of the electron beam techniques.

A second parameter that is of vital importance in surface analysis and which controls ultimate sensitivity of each characterization technique is depth of analysis. This comparison by technique is shown in Table VI and summarized in Figure 3. In Table VI the depth analyzed column gives the typical depth samples by the analytical

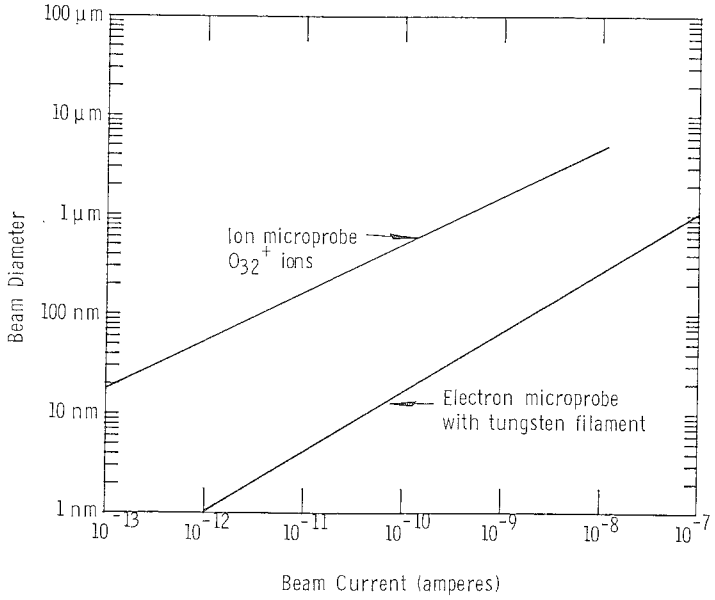

FIGURE 1 — Beam Current vs. beam diameter for the ion microprobe mass analyzer with $^{32}O+$ ions and for an electron microprobe with a tungsten filament.

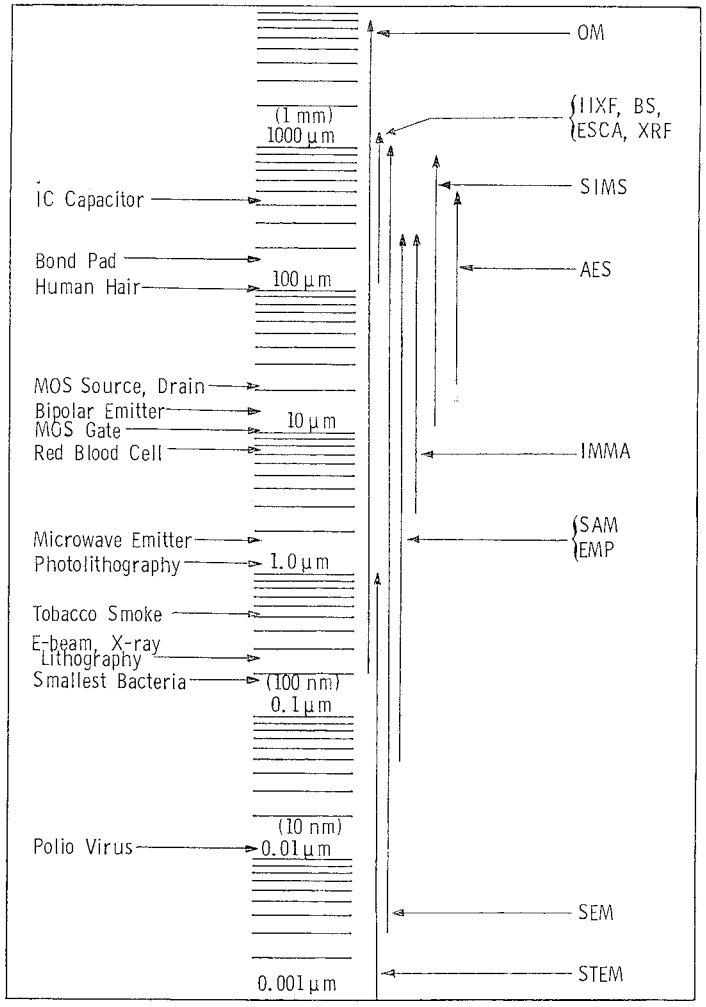

FIGURE 2 — Comparison of the diameter range of the analyzed region for various surface characterization techniques with a typical diameter or linear dimension of selected samples or materials.

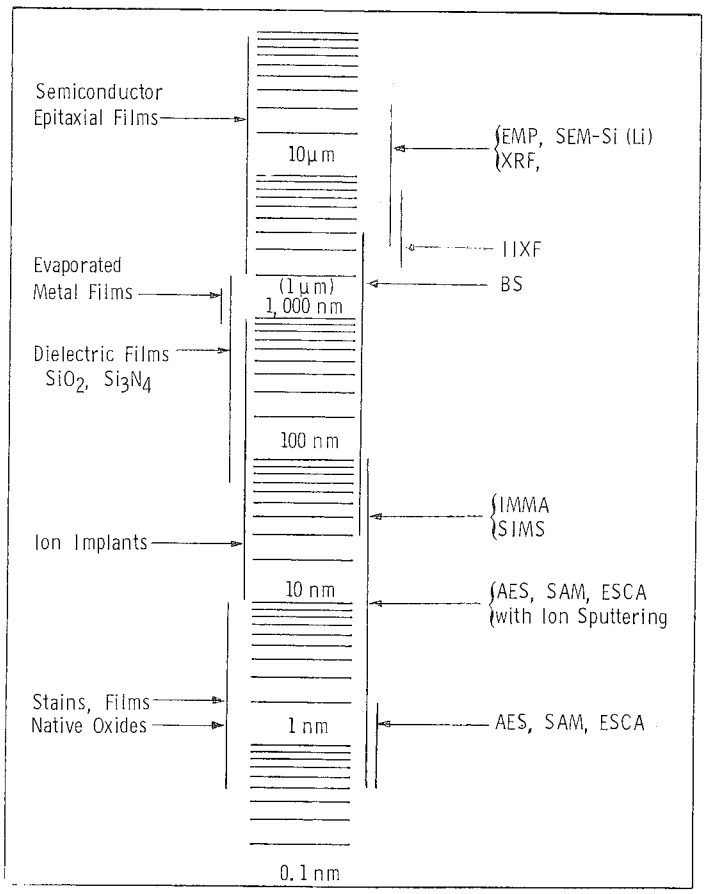

FIGURE 3 — Comparison of in-depth analytical capabilities for various characterization techniques with typical surface or film thickness on selected samples.

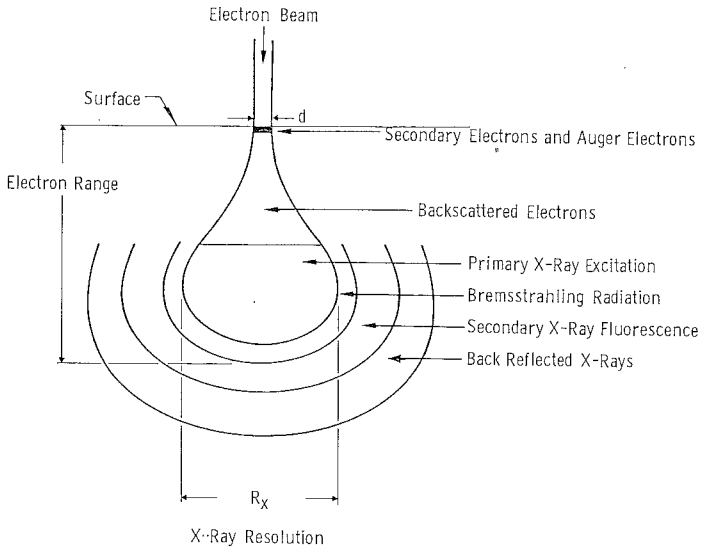

FIGURE 4 — Schematic representation of the interaction of an electron beam with a solid of moderate to low atomic number. The diameters from which x-rays are produced are shown. The primary x-ray excitation diameter R_X is a function of the electron spread diameter R and the primary beam diameter d, $R_X^2 = R^2 + d^2$.

technique. In the electron beam techniques, there is a wide range of depths sampled because of the different signals detected. This is best illustrated in Figure 4 which is an adaptation of a similar figure published by Beaman and Isasi.[7] The depth and volume analyzed are large compared to the exciting beam diameter when x-rays are detected. This is, of course, due to elastic scattering of electrons by the nuclei and the amount of scatter will be inversely proportional to the density, p, of the sample being analyzed. This spreading of the electrons and its effect on resolution has been studied by a large number of workers (see Ref. 7) resulting in an equally large numeer of formulae to calculate the extent of electron spreading and resulting x-ray spatial resolution. In this review it is not important which formula is correct since the purpose of the paper is to compare techniques and their capabilities. The formulae $R = 0.064\ E_0^{1.68}/p$ and $R_X^2 = R^2 + d^2$ have eeen chosen to illustrate the effects of sample density, p, and exciting electron energy E_0. R is the diameter of lateral electron spread, R_X is the diameter of x-ray excitation volume and d is the electron beam diameter. All diameters are in μm for these calculations. The effect of electron beam energy on depth of penetration is shown in Table VII. There is considerable penetration in the light z elements such as silicon and aluminum. The effect of this electron spreading on x-ray spatial resolution is shown in Table VIII for copper. In order to obtain submicron resolution it is necessary to work at low electron beam energies with small beam diameters. As will be pointed out later these latter two operating parameters cause degradation of other desirable analytical capabilities, e.g., detection limit, signal to noise, elements excited, etc. Another way frequently used to obtain submicron resolution is to use very thin (100-500 nm) samples which minimizes electron spreading because the scattered electrons are transmitted out the other side.

The depth of analysis of the other electron beam techniques, SEM, AES, SAM is controlled by the range of secondary electrons and Auger electrons in materials. In the case of Auger electrons the mean path in nm is approximately $0.1\sqrt{E}$ for the energy range 100 to 2000 eV.

TABLE V
DIAMETER OR WIDTH OF ANALYSIS AREA

Technique	Minimum	Range	Optimum
ELECTRONS			
AES	25 μm	25-1000 μm	100 μm
EMP	50 nm*	50 nm-100 μm	2.5 μm
SAM	50 nm	50-1000 nm	500 nm
SEM	3 nm	3-25 nm	10 nm
SEM-Si(Li)	50 nm*	50 nm-100 μm	2.5 μm
IONS			
BS	100 μm	100-1000 μm	1000 μm
IIXF	100 μm	100-1000 μm	1000 μm
IMMA	2.5 μm	2.5-250 μm	250 μm
ISS	1000 μm	1000-10,000 μm	500 μm
SIMS	15 μm	15-10,000 μm	250 μm
PHOTONS			
ESCA	1000 μm	1000-10,000 μm	10,000 μm
XRF	1000 μm	1000-10,000 μm	10,000 μm

* With thin samples

Secondary electrons average around 5 eV and are therefore highly localized around the excitation point which is why good resolution is an inherent property of the SEM.

Ion sputtering is employed as an adjunct to AES, SAM and ESCA to obtain n-depth information during surface analysis; generally 1 to 3 keV argon or krypton ions are used to sputter away the sample. Since the average Auger electron and photoelectron are emitted from a depth of 2 nm, the depth resolution for this type of analysis is the same. Sputtering as deep as 1 μm is sometimes achieved but generally most work is in the 1 to 100 nm range. SIMS, IMMA and ISS are all ion sputtering techniques and in the case of SIMS and IMMA the analytical signal is from the sputtered secondary ions. Depth resolutions of 2 nm are achievable. ISS sputtering is performed with noble ion gases and the signal is from the reflected ions. A depth resolution of 1 nm is possible.

In order to illustrate the incompatibility of maximum analytical sensitivity and minimum spatial resolution, two tables, Table IX and X, have been prepared. The data calculated for this type of comparison is fraught with disaster for the writer because every reader will be able to find exceptions for some element or matrix. Certainly, within most analytical techniques there is a wide range of elemental sensitivities for each matrix. The purpose of these calculations for these two tables is simply to compare the characterization techniques and as long as the same ground rules are used, the comparisons are valid and can illustrate the advantages and disadvantages of each technique. In these two tables the calculations were all based on silicon. The assumptions used for analytical volume calculations are shown with the tables.

TABLE VI
DEPTH ANALYZED, DEPTH RESOLUTION AND DEPTH RANGE

Technique	Depth Analyzed	Atomic Layers	Resolution	Range
ELECTRONS				
AES	0.5-2 nm	1-5	1 nm	1nm-1 μm*
EMP	1-25 μm	10^4-10^5	Limited	Limited
SAM	0.5-2 nm	1-5	1 nm	1 nm-1 μm*
SEM	2.5-5 nm	2-10	3 nm	none
SEM-Si(Li)	1-25 μm	10^4-10^5	Limited	Limited
IONS				
BS	0.03-3 μm	5	20 nm	0.03-3 μm
IIXF	1-5 μm	10^4	Limited	Limited
IMMA	0.5-2 nm	10^3-10^4	2 nm	2 nm-1 μm*
ISS	0.5-2 nm	1-2	1 nm	1 nm-1 μm*
SIMS	0.5-2 nm	1-5	2 nm	2 nm-1 μm*
PHOTONS				
ESCA	0.5-2 nm	1-5	1 nm	1 nm-1 μm*
XRF	3-25 μm	10^4-10^5	Limited	Limited

* With ion sputtering

TABLE VII
EFFECT OF ELECTRON BEAM ENERGY ON ELECTRON SPREAD

Electron Beam Energy kV	Electron Spread or Penetration, μm Silicon	Copper	Gold
5	0.4	0.1	0.05
10	1.3	0.3	0.2
20	4.2	1.1	0.5
30	8.4	2.2	1.0

TABLE VIII
EFFECT OF BEAM DIAMETER ON
X-RAY RESOLUTION FOR COPPER

Electron Beam Energy kV	X-Ray Resolution, μm — 0.1 μm Beam	1 μm Beam	5 μm Beam
5	0.14	1.0	5.0
10	0.3	1.0	5.0
20	1.0	1.4	5.1
30	2.2	2.4	5.5

Table IX shows the necessary matrix volume and associated analytical diameter necessary to achieve the minimum detection limits for each characterization technique. Notice that the diameters of all the analyzed areas are larger than the 10 μm diameter earlier defined as the maximum diameter for microanalysis. The absolute detection limit expressed as grams or atoms varies by a factor 10^8 depending on the analytical technique. The IMMA, SAM, and SIMS show very high absolute sensitivity $\simeq 10^5$ to 10^6 atoms. The same three techniques show strikingly different detection limits when the analytical volume is taken into consideration and concentrations are considered, i.e., SAM vs. IMMA. The volume of material required by each analytical technique is similarly quite different, e.g., 8×10^{-4} cc for XRF compared to 2×10^{-15} cc for SAM. This volume difference is, of course, reflected in the diameter of the analysis area (last column in Table IX).

Table X shows what detection limit can be expected when the beam diameter or diameter of the area analyzed is at the minimum or best that the technique is capable of achieving. As can be seen, there are significant differences in detection limits from the minimum values given in Table IX. The reason for this degradation in detection is readily understood when the volumes analyzed are compared in Tables IX and X. The sensitivities of each characterization technique remain the same but the minimum detectable concentrations increase with decreasing analytical volume. From these data, it is apparent that microanalysis is not compatible with trace analysis. Conversely, trace analysis and microanalysis are mutually exclusive. Therefore, in surface characterization, there must always be a trade-off between the two goals to obtain the best solution for each analytical problem. It is unrealistic to believe that ppm sensitivity can be achieved in the analysis of a 2 nm thick surface with 1 to 10 μm lateral resolution.

TABLE IX
MAXIMUM SENSITIVITY AND ASSOCIATED ANALYTICAL VOLUME AND PROBE DIAMETER

Technique	Detection Limit, ppma	Min. Detection Limit Atoms	Grams	Vol., cc Analyzed	Diam. Analyzed
ELECTRONS					
AES	1000-10,000	2×10^{9}	1×10^{-13}	1×10^{-10}	250 μm
EMP	100-10,000	2×10^{10}	8×10^{-13}	8×10^{-9}	25 μm
SAM	1-50%	3×10^{5}	2×10^{-17}	2×10^{-15}	1 μm
SEM-Si(Li)	100-10,000	2×10^{10}	8×10^{-13}	8×10^{-9}	25 μm
IONS					
BS	100-10,000	2×10^{11}	8×10^{-12}	8×10^{-8}	0.1 cm
IIXF	1-100	4×10^{10}	2×10^{-12}	2×10^{-6}	0.1 cm
IMMA	0.01-100	1×10^{5}	5×10^{-18}	2×10^{-10}	150 μm
ISS	10,000	2×10^{13}	1×10^{-9}	4×10^{-9}	0.1 cm
SIMS	0.1-1000	2×10^{6}	1×10^{-16}	5×10^{-10}	250 μm
PHOTONS					
ESCA	1000-10,000	3×10^{12}	2×10^{-10}	2×10^{-7}	1 cm
XRF	1-100	2×10^{13}	8×10^{-10}	8×10^{-4}	1 cm

Assumptions used for calculating volume analyzed:
AES — 2 nm x 250 μm dia.
EMP and SEM-Si(Li) — 25 μm dia. sphere.
SAM — 2 nm x 1 μm dia.
ESCA — 2 nm x 1 cm dia.
XRF — 10 μm x 1 cm dia.
BS — 100 nm x 0.1 cm dia.
IIXF — 2.5 μm x 0.1 cm dia.
ISS — 5 nm x 0.1 cm dia.
IMMA — 10 nm x $(150\ \mu m)^2$.
SIMS — 10 nm x 250 μm dia.

TABLE X
MINIMUM SAMPLE DIMENSIONS: VOLUME, WEIGHT, ATOMS AND ASSOCIATED DETECTION LIMITS

Technique	Beam Diameter	Vol., cc Analyzed	Grams Analyzed	Atoms Analyzed	Detection Limit
ELECTRONS					
AES	25 μm	1×10^{-12}	2×10^{-12}	5×10^{10}	5-50%
EMP	50 nm	1×10^{-12}	2×10^{-12}	5×10^{10}	2-20%
SAM	100 nm	2×10^{-17}	4×10^{-17}	8×10^{5}	20-100%
SEM-Si(Li)	50 nm	1×10^{-12}	2×10^{-12}	5×10^{10}	2-20%
IONS					
BS	100 μm	2×10^{-10}	4×10^{-10}	8×10^{12}	1-10%
IIXF	100 μm	2×10^{-8}	5×10^{-8}	1×10^{15}	0.01-0.1%
IMMA	2.5 μm	1×10^{-14}	2×10^{-14}	5×10^{8}	0.2-20%
ISS	0.1 cm	4×10^{-10}	1×10^{-9}	2×10^{13}	10-100%
SIMS	15 μm	4×10^{-13}	8×10^{-13}	8×10^{10}	1-20%
PHOTONS					
ESCA	0.1 cm	2×10^{-9}	4×10^{-9}	1×10^{14}	5-50%
XRF	0.1 cm	8×10^{-6}	2×10^{-5}	4×10^{17}	100-1000 ppm

Assumptions used for calculating volume analyzed:
AES - 2 nm x 25 μm dia.
EMP and SEM-Si(Li) — 10 kV beam, 1.3 μm dia. sphere.
SAM — 2 nm x 100 nm.
ESCA — 2 nm x 0.1 cm dia.
XRF — 10 μm x 0.1 cm dia.
BS — 20 nm x 100 μm dia.
IIXF — 2.5 μm x 100 μm dia.
ISS — 0.5 nm x 0.1 cm dia.
IMMA — 2 nm x 2.5 μm dia.
SIMS — 2 nm x 15 μm dia.

Figure 5 is a summary of the data given in Tables IX and X. It is a graphic representation of the detection limit for each characterization technique as a function of the diameter of the area analyzed. For each technique, when the smallest diameter is reached, the detection limit quickly approaches 100%. Proceeding in the other direction, when the largest diameter is reached, the best or optimum detection limit has been reached. Providing a larger sample serves no useful purpose because the technique is not capable of analyzing a larger area. Notice that there are no techniques capable of detecting 1 ppm with a 1 μm diameter beam. The left side of this Figure clearly shows the absence of any analytical techniques with sub-micron resolution and ppm detection limits.

Elemental coverage, specificity and the variation of sensitivity between elements is summarized in Table XI.[3] AES, SAM, and ESCA have excellent elemental coverage,

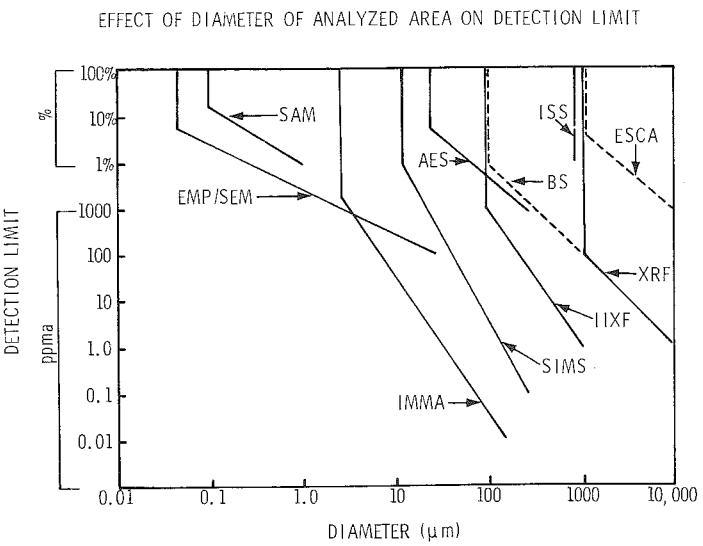

Figure 5.

from lithium through uranium. The Auger de-excitation process competes with x-ray emission in all excited atoms; with 90% probability for Auger emission in the light elements falling to 50% probability around arsenic, and 10% probability from the heavy z elements. This means that the sensitivity in AES and SAM varies by less than a factor of 10 throughout the periodic table. ESCA shows a similar uniformity in sensitivity. Elemental coverage and specificity tend to be detector limited in the x-ray techniques. When wavelength dispersive detectors are employed (EMP and XRF) the light elements B through Mg can be determined. However, if a solid state Si(Li) detector is used (SEM-Si(Li) and IIXF) then the beryllium window absorbs the x-rays from these light elements. Elemental specificity is also affected by x-ray detector choice. Natural line widths for x-ray emission are around 0.5 eV. Typical wavelength detector resolutions are 1 to 10 eV over the operating range while the solid sate detectors, Si(Li), have resolutions at best of 145-150 eV at 5.9 keV x-rays and are somewhat worse at higher energies. As a result, both signal to noise and elemental selectivity (resolution) are significantly better for wavelength dispersive detectors. However, energy dispersive detectors intercept a solid angle several hundred times larger than the crystal spectrometer collimator. Therefore, data state detectors, higher sensitivities are attainable and the electron probes can be operated at lower beam currents ($10^{1}w^{11}$ amps) to minimize sample damage.

Backscattered ion spectroscopy or Rutherford scattering works best for high z elements in a low z matrix. While sensitivity increases with higher z, specificity or resolution increases with smaller z because the energy, E, of the backscattered ion is controlled by the difference in mass between the bombarding ion, M, and target ion, m, Equation 1.

$$E = \left[\frac{M - m}{M + m}\right] E_0^2 \qquad (1)$$

The determination of light z elements in a heavy matrix is very difficult because the backscattered peak lie on a high, broad continuum of backscattered ions from the matrix.

There are a number of factors which enter into a comparison of surface characterization techniques that are difficult to quantitate. This type of comparison serves a useful function in helping to choose an analytical technique to solve a specific problem, e.g., accuracy, availability of standards, non-destructiveness, in-depth profiling capability, etc. Tables XII and XIII answer many of these questions and are, in general, self-explanatory. Estimates of precision and accuracy in Table XII probably are on the conservative side. All techniques can be made quantitative if standards are available. Good standards for surfaces do not exist and are difficult to envision. Most electron beam excitation techniques are non-destructive to metal samples but can cause chemical changes in organic samples. Many inorganic samples will undergo chemical decomposition during intensive electron bombardment. All in-depth profiling techniques are destructive when ion sputtering is employed. Crater wall rejection is an important consideration during in-depth profiling. This is accomplished in IMMA by electronic gating, in SIMS using apertures and in AES and SAM by using a small electron probe in the center of a large ion sputtered crater.

In the analysis of surfaces with ion or electron beams, sample charging can be a problem. Generally only insulators or high resistivity samples charge up. When this occurs the beam is deflected from the sample and micropositioning of the beam as well as x-y imaging are virtually impossible. Coating of the sample with a thin layer of carbon, gold or other metal can go a long way toward alleviating this problem. In ISS the charging problem is minimized using an electron gun to flood the sample surface with electrons. IMMA and SIMS use negative sputter ions to analyze samples with charging problems although there is considerable reduction in analytical sensitivity. X-ray excited techniques, ESCA and XRF, generally do not have this problem.

As has become apparent in this review, there is a constant trade off in analytical capability within any technique depending on the needs of the analyst. Tables XIV and XV summarize the expected effects of the analytical capability when changes are made in selected operating parameters for electron beam, SEM/EMP, and ion beam, IMMA/SIMS, techniques. In Table XIV, it is assumed that a combination SEM/EMP instrument is in use. Most items in the table are readily understood. The role of increasing accelerating voltage on the detection limit is complex. The excitation energy must be greater than the binding energy of the electron to create an excited atom. At the same time an increase in accelerating voltage will cause both an increase in bremsstrahlung (lower signal to noise) as well as generation of x-rays at greater depths in the sample. The amount of bremsstrahlung increases in proportion to z. In the electron microprobe analysis for a low z element, e.g., carbon, an increased accelerating voltage will be detrimental because the carbon x-rays will be generated too deeply in the sample to escape and those that do escape will be lost in the increased background or bremsstrahlung radiation.

TABLE XI
ELEMENTAL COVERAGE, SPECIFICITY AND SENSITIVITY VARIATION

Technique	Coverage	Specificity	Sensitivity Variation*
ELECTRONS			
AES	Li-U	Good	Varies by less than factor of 10
EMP	B-U	Good	Wide (10^3), depends on exciter and detector
SAM	Li-U	Good	Varies by less than factor of 10
SEM-Si(Li)	Mg-U	Medium	Wide (10^3), depends on exciter and detector
IONS			
BS	Li-U	Lo Z Good, Hi Z Poor	Increases with Z, Bi/O = 100
IIXF	Mg-U	Medium	Wide (10^3) depends on exciter and detector
IMMA	Complete	Good	Wide (10^4-10^5), depends on ionization efficiency
ISS	Li-U	Lo $\frac{M}{m}$ Good, Hi $\frac{M}{m}$ Poor	Increases with Z, Bi/O = 5
SIMS	Complete	Good	Wide (10^4-10^5) depends on ionization efficiency
PHOTONS			
ESCA	Li-U	Good	Varies by less than factor of 10
XRF	B-U	Good	Wide (10^3), depends on exciter and detector

Therefore, both the matrix and element being sought must be considered and the accelerating voltage adjusted to optimize analytical sensitivity.

Table XV lists the ion beam parameters and their effects upon analytical capability. As can be seen, the same basic trade-offs occur, i.e., increasing beam current improves the detection limit but degrades analytical resolution.

Summary

Techniques for the characterization of solid surfaces have been divided into two categories. One category includes techniques which are used to image or measure the microtopography of a surface and to characterize defects in the surface. The second category covers the techniques used for chemical characterization of surfaces. The choice of techniques for this review was based on the breadth of application, maturity and commercial availability for each surface characterization technique.

In surface topography the capabilities of optical microscopy, optical interferometry, profilometry, electron microscopy and scanning electron microscopy are covered. While optical microscopy and the SEM are widely used for lateral, x-y, characterization, the profilometer and optical interferometry are used for vertical, z, characterization. Microdefects are characterized by electron diffraction, optical microscopy, SEM and x-ray diffraction.

Techniques used for chemical characterization of solid surfaces have been divided into three categories based on the excitation process: electrons, ions and photons. The electron beam techniques excel in spatial resolution and have excellent imaging capabilities. The ion beam techniques have good in-depth, z, profiling capability and the ion microprobe and secondary ion mass spectrometer have outstanding sensitivity for many elements. The incompatibility of trace analysis and microanalysis is clearly demonstrated. Using currently available characterization techniques, it is not possible to simultaneously obtain micrometer spatial resolution and ppm sensitivity. There is a trade off in each analysis of elemental sensitivity for spatial resolution.

The complete characterization of a surface is the consolidation of the results from a number of characterization techniques. The results of imaging, microtopography, chemical analysis in the lateral, x-y, and vertical, z, directions must be correlated to obtain a coordinated characterization of the surface.

Acknowledgements

The cooperation of Dr. D. Wittry and particularly Dr. C. A. Evans, Jr., in supplying reprints and suggestions is deeply appreciated. Much of the data reported comes from Dr. Evans' publications. Dr. Robert Dobrott was of great help in checking the data in many of the tables. John Devanee and Kathy Leedy suggested the format and provided some of the data for Tables XIV and XV.

References

1. Materials Advisory Board, **Characterization of Material** (Publication MAB-229-M), Clearinghouse for Federal Scientific and Technical Information, Springfield, Virginia, U.S.A., 1967, I-ix.
2. P. F. Kane and G. B. Larrabee, **Characterization of Solid Surfaces,** Plenum Press, N.Y., U.S.A., 1974, 1-5.
3. C. A. Evans, Jt., "Surface and Thin Film Compositional Analyeis", Anal. Chem., 47, 1975, 818A-829A.
4. C. A. Evans, Jr., "Surface and Thin Film Analysis," Anal. Chem., 47, 1975, 855A-866A.
5. J. W. Mayer and A. Turos, "Comparison of Surface Layer Analysis Techniques," Thin Solid Films, 19, 1973, 1-10.
6. D. B. Wittry, "Micro-analysis-Past, Present, Future", **Proc. of Advanced Techniques in Failure Analysis,** IEEE, Newport Beach, Cal., U.S.A., 1-8.
7. D. R. Beaman and J. A. Isasi, "Electron Beam Microanalysis — Part I", Mater, Res. Stand., 11, 1971, 8-78.

TABLE XII
PRECISION, ACCURACY, TECHNIQUE COSTS AND ANALYSIS TIME

Technique	Quantitative	Standards Available	Reproducibility	Accuracy	Cost ($K)	Analysis Time (Min.)
ELECTRONS						
AES	Semi	No	± 20	± 100	50	30
EMP	Yes	Yes	± 2	± 5	150	120
SAM	No	No	± 20	± 100	200	120
SEM-Si(Li)	Yes	Yes	± 2	± 5	50	15
IONS						
BS	Yes	Internal	± 10	± 5	125	180
IIXF	Semi	Some	± 20	± 30	125	180
IMMA	Semi	No	± 10	± 100	250	30
ISS	Semi	No	± 20	± 100	50	180
SIMS	Semi	No	± 10	± 100	100	30
PHOTONS						
ESCA	Semi	No	± 25	± 100	100	180
XRF	Yes	Yes	± 1	± 5	50	15

TABLE XIII
CAPABILITIES, PROBLEMS AND LIMITATIONS

Technique	Sample Charging	Sample Sputtering	Beam Induced Chem. Chg.	Z Profiling	X-Y Imaging Resolution	Crater Wall Rejection
ELECTRONS						
AES	Yes	No*	Yes	No*	No	Yes
EMP	Yes	No	Yes	No	100 nm	—
SAM	Yes	No*	Yes	No*	100 nm	Yes
SEM-Si(Li)	Yes	No	Yes	No	100 nm	—
SEM	Yes	No	Yes	No	3 nm	—
IONS						
BS	No	No	No	Yes	No	—
IIXF	No	Yes	Yes	No	No	—
IMMA	Yes	Yes	Yes	Yes	2-10 μm	Yes
ISS	No	Yes	Yes	Yes	1 nm	Fair
SIMS	Yes	Yes	Yes	Yes	2-25 μm	Yes
PHOTONS						
ESCA	No	No*	No	No*	No	No
XRF	No	No	No	No	No	—

* Yes, with ion sputter gun in system

TABLE XIV
SEM/EMP — ELECTRON BEAM PARAMETER EFFECTS

	Increasing Accelerating Voltage	Increasing Beam Current	Increasing Beam Diameter	Increaing Specimen Tilt	Coating Specimen
BEAM PENETRATION	Increase	—	—	Decrease	Decrease
SIGNAL TO NOISE RATIO	Decrease	Increase	Increase	Increase	Increase
SEM RESOLUTION	Improve	Degrade	Degrade	Improve	Degrade

TABLE XIV CONTINUED

	Increasing Accelerating Voltage	Increasing Beam Current	Increasing Beam Diameter	Increasing Specimen Tilt	Coating Specimen
CONTRAST	Decrease	Increase	Decrease	Increase	Increase
CHARGING	Sample dependent	Increase	—	Decrease	Decrease
CONTAMINATION DUE TO BEAM	Increase	Increase	—	—	—
DETECTION LIMIT	Complex	Improve	Improve	Degrade	Degrade
EMP RESOLUTION	Degrade	Degrade	Degrade	Degrade	Degrade

TABLE XV
IMMA/SIMS — ION BEAM PARAMETER EFFECTS

	Increasing Accelerating Voltage	Increasing Beam Current	Coating Specimen	Increasing Beam Diameter
SPUTTER RATE	Decrease	Increase	—	Decrease
SIGNAL TO NOISE RATIO	Decrease	Increase	—	Increase
ANALYTICAL RESOLUTION	Improve	Degrade	Improve	Degrade
IMAGE CONTRAST	Decrease	Increase	Increase	Decrease
CHARGING	Increase	Increase	Decrease	Increase
DETECTION LIMIT	Degrade	Improve	—	—

EM Short Courses

SCANNING ELECTRON MICROSCOPY AND X-RAY MICROANALYSIS. June 13-17, 1977, Lehigh University, Bethlehem, Pa., Tuition $375.

Lecturers: Patrick Echlin, Joe Goldstein, David Joy, Eric Lifshin, Dale Newbury, Harvey Yakowitz. Coverage: Fundamentals of SEM and Electron Microprobe, Solid State X-ray Detector, Quantitative X-ray Analysis, Preparation of Biological Specimens, Scanning Transmission Electron Microscopy (STEM). Laboratories: Four SEM instruments, one automated electron microprobe, and one STEM instrument will be used in the laboratory sessions. A solid state detector is available with each of these electron beam instruments. Information and Registration Forms available from: Professor J. I. Goldstein, Department of Metallurgy & Materials Science, Whitaker Lab No. 5, Lehigh University, Bethlehem, Pa. 18015.

SCANNING AND TRANSMISSION ELECTRON MICROSCOPY. A series of practical courses will be offered during June 1977. Transmission Electron Microscopy — June 6-17. Scanning Electron Microscopy — June 20-24 and June 27-July 1.

These classes are designed to introduce the participants to the theory and practical aspects of electron microscopy. Primary emphasis will be on specimen preparation, operation of electron microscopes, and photographic and darkroom techniques. Tuition will be $500 for TEM, $425 for SEM, and $800 for the combined program.

For information, write or call: Fred Lightfoot, Department of Anatomy, George Washington University, 2300 "I" Street, N.W., Washington, D.C. 20037. (202) 676-2881 or 3511.

INTENSIVE TWO-WEEK TRAINING SESSION IN TRANSMISSION AND SCANNING ELECTRON MICROSCOPY. Includes Freeze-Etch Replication Techniques, EM Autoradiography and X-Ray Microanalysis. September 4-16, 1977, Duke University Marine Laboratory, Beaufort, N.C. 28516. Dr. John D. Costlow, Director.

Staff of internationally recognized experts in specialized techniques. Wide variety of instruments and equipment available for use by participants. Course geared to research investigators, but technicians and advanced graduate students are also invited to apply.

For descriptive brochure and application form, write to: Dr. Eve L. MacDonald, Program Coordinator, Electron Microscope Institute, Duke University Marine Laboratory. Mailing address: Department of Toxicology and Experimental Pathology, Burroughs Wellcome Co., 3030 Cornwallis Road, Research Triangle Park, North Carolina 27709.

Can You Use Maximum Resolution?

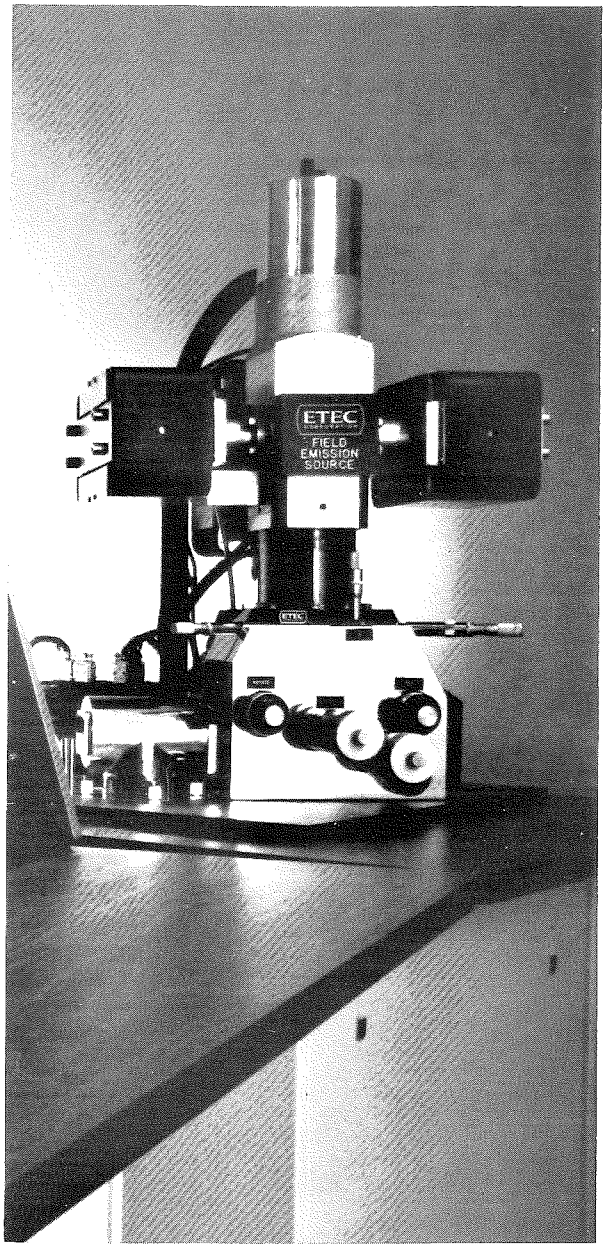

ETEC's Field Emission Electron Source System

- **Routine high resolution**
- **High stability**
- **Standard SEM vacuum in the specimen chamber**
- **Slow scan image recording possible**
- **Easily operated**

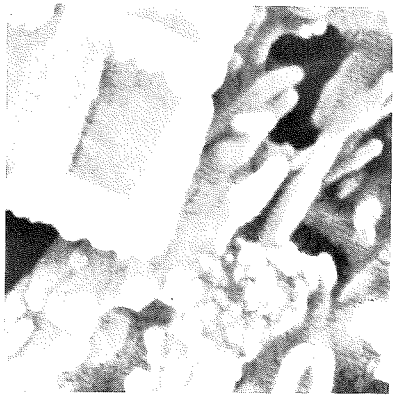

Fullam Resolution Sample
55,000X
20kV, 0° Tilt

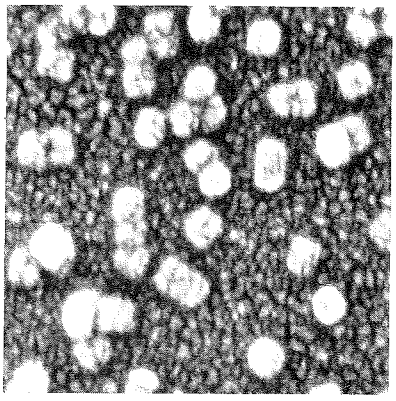

Hemocyanin Molecules
110,000X
20kV, 0° Tilt

ETEC CORPORATION
3392 Investment Boulevard
Hayward, California 94545

Application/Nomination For Membership

I hereby apply/nominate for Regular ☐ Student ☐ Corporate ☐ membership in the Texas Society for Electron Microscopy.

Name of institution applicant or corporation nominee person _____

P. O. Address _____

_____

Information as to position, degrees, and qualifications for Membership: _____

_____

_____

_____

This nomination is accompanied by a statement of interest in and contributions to Electron Microscopy and associated fields of science.

One year's dues in the form of a check or money order should be sent with the application for Membership form. (Regular $5.00, Student $1.00, Corporate $50.00)

Signature of one Member making the nomination:

_____

Dated _____ 19 _____

This application to Membership in the Society, or this application for transfer from the grade of Student to Regular Member, signed by one Member should be sent to the Secretary to be presented at the next meeting of the Council or approval by a majority vote of the Council. Notice of approval will be mailed by the Executive Secretary.

_____

Presented to the Council at _____ meeting. Date _____

Action _____

Remarks _____

Send Application to: Dr. Richard Hillman, Sec.
Department of Anatomy
Texas Tech University School of Medicine
Lubbock, TX 79409

Quantitatively Speaking About Column Applications ...PGT has something to say

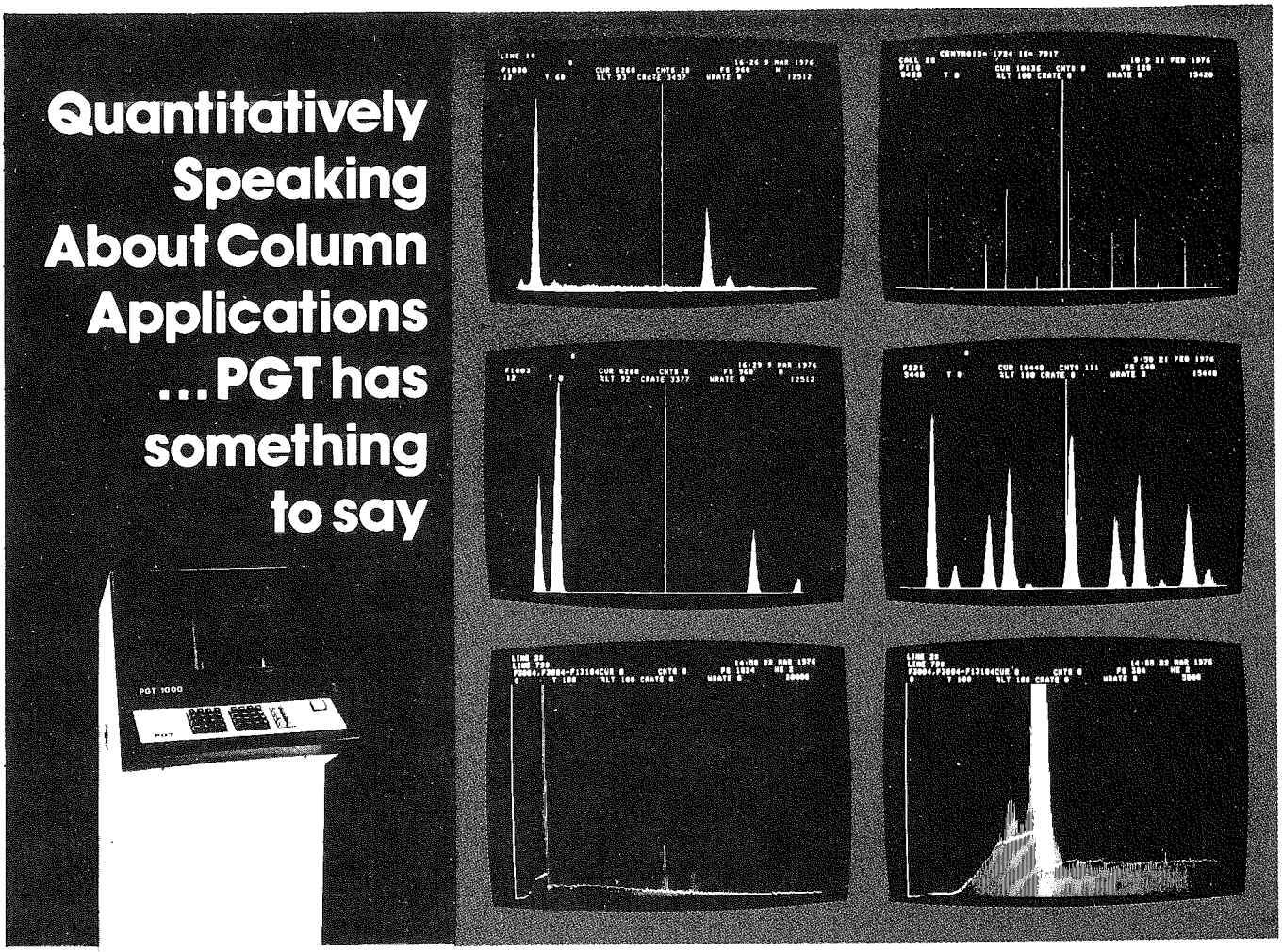

With the PGT quantitative microanalysis system you get:

- ☐ The PGT-1000 Multichannel X-ray Analyzer with keyboard controls for ease-of-operation and 12-inch video screen for alphanumeric and spectral display
- ☐ a Dual Floppy Disc system which provides
  - modern, mass data storage and
  - rapid access to stored information
- ☐ a quantitative program that takes into account all major analytical factors—background (including absorption edges), peak overlap, window absorption and Si(Li) escape peaks
- ☐ the most advanced quantitative algorithm available to give you increased accuracy
- ☐ a Si(Li) detector with PGT's unique detector mount featuring variable Z motion and vernier retraction
- ☐ technical support from PGT's applications laboratory
- ☐ a full one year warranty on all systems including the computer

If your current application does not require a quantitative system—consider the PGT-1000 computer-based qualitative system. It's competitively priced with hard-wired analyzers and is easily converted to quantitative applications.

Call today and arrange for a demonstration of the PGT-1000 microanalysis system in our Princeton Applications Laboratory.

PGT
PRINCETON GAMMA-TECH

Box 641 • Princeton, N.J. 08540 • Tel: 609 924-7310 • Cable PRINGAMTEC • Telex: 843486

The new LKB UM IV Ultrotome® has something special for everyone.

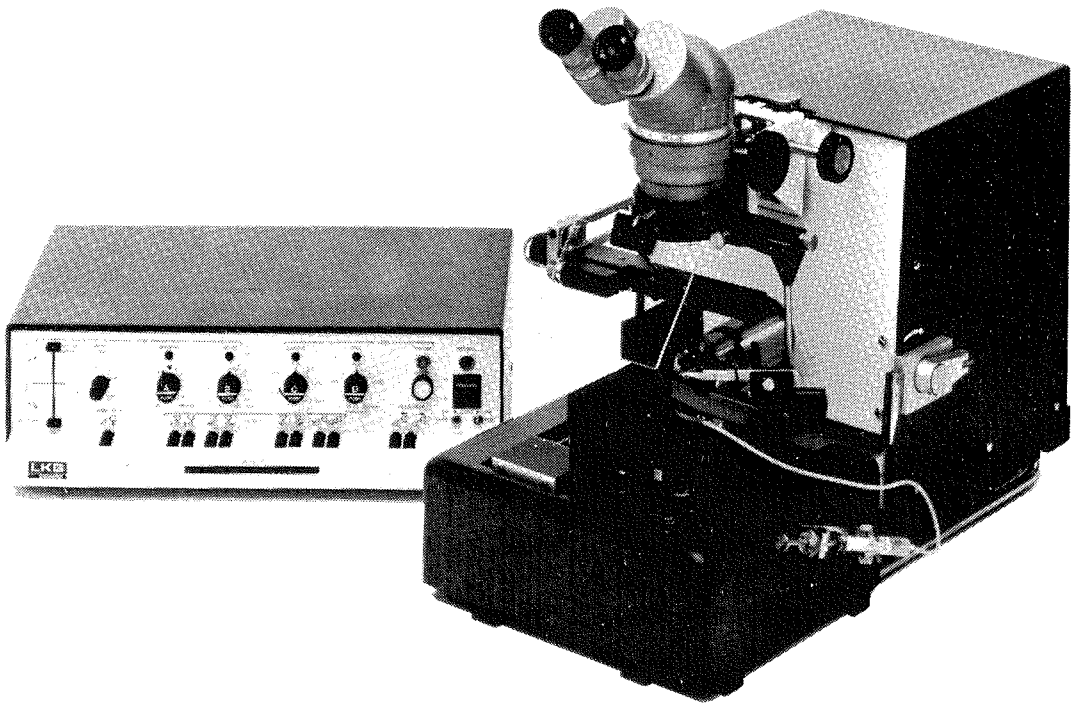

— It is an ultramicrotome which also includes a microtome function for the cutting of semithin sections in the 0.2 - 2.5 μm range.

— LKB UM IV is the only ultramicrotome which has complete push-button automation of knife stage movements.

— »Automatic» machine trimming produces rapid and precise pyramids and mesas.

— Highly versatile orientation head allows you to section in the specimen plane of your choice.

— Unique structure viewer (with face-on and top view) for precise localization and structure observation before and during sectioning.

— A new impulse controlled thermal feed system with a memory function. This allows you to stop and restart without loss of valuable material. It also ensures the highest reproducibility in section thickness.

— When trying the UM IV you will discover a new world of speed and precision in obtaining sections ..... and be amazed by the extreme ease of operation. And there are many more new features which will bring outstanding benefits to your laboratory. Send for complete information today.

LKB UM IV for better sections, in a more convenient way!

LKB

LKB Instruments Inc.
12221 Park Lawn Drive, Rockville, Md 20852
tel: (301) 881-2510, telex: 230 89 682.

Penetration of Heavy Metal Stains Into Thin Sections

How far into thin sections do metal ions penetrate for tissue staining? Do the ions migrate throughout the sections and stain all tissue elements or is thin section staining simply a surface effect with metal deposition only on the face of the section? We became interested in this question when trying to interpret ultrastructural detail in thin plastic sections containing various cellular structures. The answer is most important in morphometric analysis, in interpretation of stereo pairs, in serial section reconstructions, and simply in interpretation of fine ultrastructural details.

The classical EM textbooks offer conflicting views on the issue. Both Pease[1] and Hayat[2] imply, without specific statements, that the metal stains penetrate the plastic thin sections. Sjostrand[3] on the other hand states that "a very thin surface layer is stained", using the unpublished work of Maunsbach[4] on vestopal sections as a reference.

There is little recent work on stain penetration to be found in the literature. The existing reports (5-10) each deal with different plastics, different stains and staining procedures, and different methods of study (i.e. varying section thickness, use of stereo pairs, transverse sectioning of reembedded stained sections). Thus only their conclusions can be compared. All of the reports we found use osmium tetroxide as a postfixative after aldehyde fixation. This confuses the interpretation of results because the degree of staining that osmium gives to the tissue obscures the assessment of the degree of staining caused by the thin section staining. We have omitted osmium postfixation in our own studies involving stereo pairs (GMW & ILC) and reembedded stained sections (GSK & ILC). We can therefore add somewhat to the overall story.

Other than Maunsbach's[4] unpublished (uncriticizeable) work, the literature is in agreement that structures in a thin section are stained both on the surface and below the surface, commonly to at least a depth of 100 nm, the thickness of a gold section, using staining durations of 10 minutes or more. Our results concur. However Hayden[9,10] as well as Gray and Willis[6] conclude that the stain on the surface has more image contrast than stain embedded in the section. This can create problems of interpretation depending upon the extent of the difference in contrast.

The manner in which stain penetrates thin sections is open to question. Shalla[8] reported that the stain penetrates only when a structure (tobacco mosaic virus, TMV, in his work) intercepts the surface when maraglass plastic is used as the embedment but that a structure surface intercept is not needed when the TMV is embedded in methacrylate. The suggestion is that the stain doesn't diffuse through the epoxy plastics but rather migrates along channels associated with tissue ultrastructure and can only reach those structures when they are continuous to the surface. Thus under Shall's concept, some subsurface structures may not become stained at all. Structures without continuity to the surface may be overlooked during counts for morphometric analysis. Our observations of transverse sections of a sandwich of reembedded stained and unstained sections are equivical. Some subsurface structures are not stained but there is no pattern to the results. For example, in some liver tissue that we used in this manner, we found that some of the subsurface glycogen stained and some did not. It is possible that the unstained glycogen had no tissue channel pathway to the surface whereas the stained glycogen did.

Therefore questions remain. How does the stain penetrate the section (via channels or via diffusions through the plastic)? Are there types of ultrastructures which do not stain or stain variably? What is the rate and extent of stain penetration for various plastics, stains, and staining methods?

We offer the following staining recommendations: (1) One should not assume that only the most superficial (10 nm) structures stain nor that all structures in the section stain, (2) for morphometric or stereoscopic analysis, serial section, or stereological work it is best to do **en bloc** staining with uranyl acetate, because it may be that all structures do not stain when one stains only thin sections, (3) very thin sections (grey interference color) are recommended for study of ultrastructural (1-5 nm diameter) details because of the lesser possibility for superimposition of structures and the enhanced contrast of surface deposited stains.

I.L. Cameron and G.W. Williams
Dept. of Anatomy, South Texas Medical Center, San Antonio, Texas

G.S. Kirby, I. Chen, and B. Cohn
Dept. of Anatomy, Tulane Medical Center
New Orleans, La.

1. Pease, Daniel, C. **Histological Techniques For Electron Microscopy,** Academic Press, New York, 1964.
2. Hayat, M.A. **Principles and Techniques of Electron Microscopy, Volume 1,** Van Nostrand Reinhold Co., New York, 1970.
3. Sjostrand, F.S. **Electron Microscopy of Cells and Tissues, Volume 1,** Academic Press, New York, 1967.
4. Maunsbach, A.B. cited in and (3)p. 298.
5. Peters, A., Hinds, P.L., Vaughn, J.E. Extent of stain penetration in sections prepared for electron microscopy. J. Ultrast. Res. **36**:37-45, 1971.
6. Gray, E.G. and Willis, R.A. Problems of electron stereoscopy of biological tissue. J. Cell Sci, **3**:309-26, 1968.
7. Willis, R.A. end Gray, E.G. Electron stereoscopy of tissue sections. J. Anat. **100**:690, 1966.
8. Shalla, T.A., Caroll, T.W., and De Zoeten, G.A. Penetrations of stain in ultrathin sections of Tobacco Mosaic Virus. Stain Technol, **39**:257-65, 1964.
9. Haydon, G.B. Electron phase and amplitude images of stained biological thin sections. **J. Micros. 89,Pt 1**:73-82, 1969.
10. Haydon, G.B. An electron-optical lens effect as possible source of contrast in biological preparations. J. Micros. **90**: 1-13, 1969.

Analytical Research Services

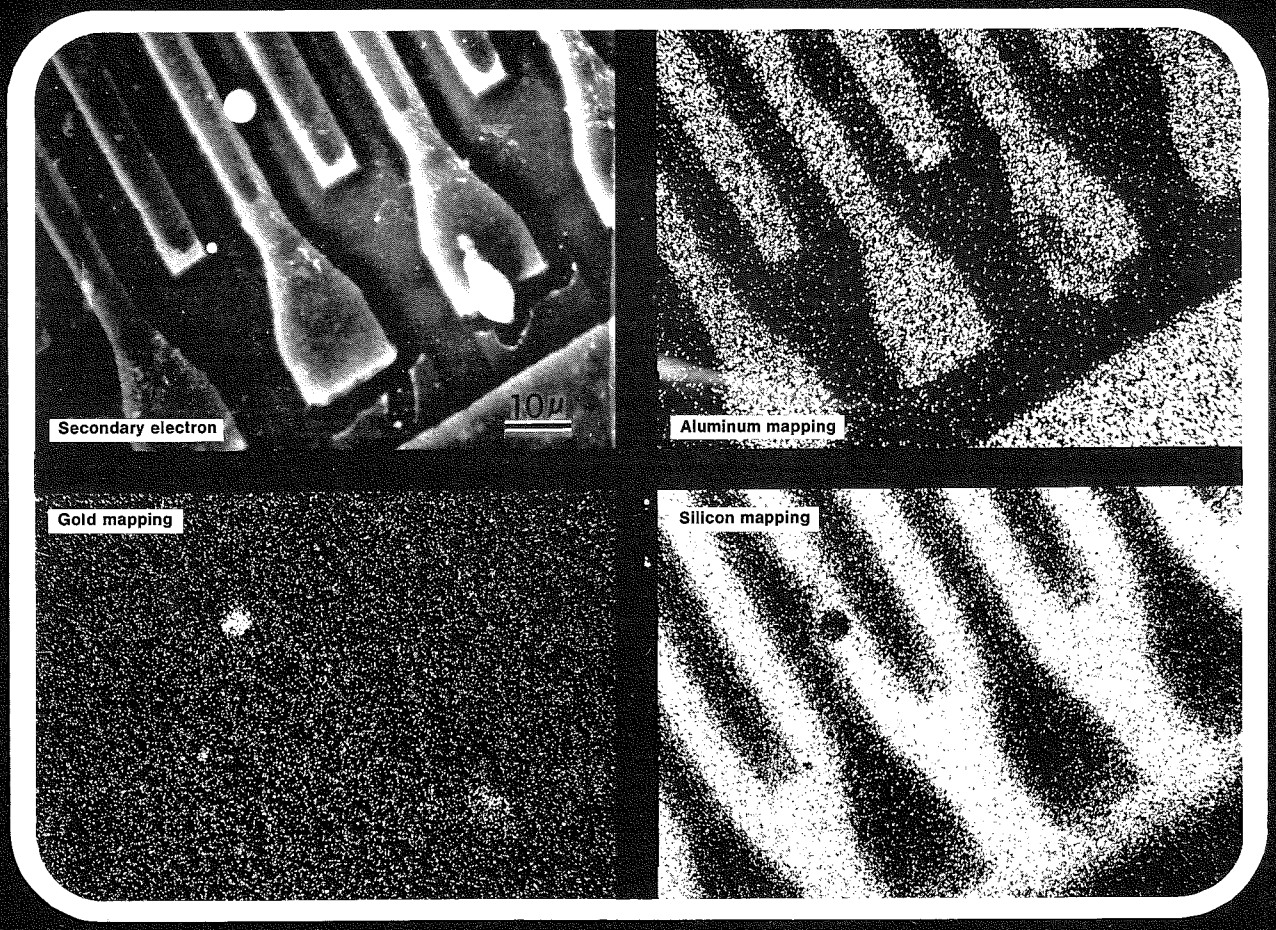

Identification of sub-micron size particulate contaminants during a failure analysis of a microelectronic device

Scanning Electron Microscopy
Two High Resolution SEM's with Television Scan, Video Tape Recorder, Tensile Stage, High Temperature (to 1600°C) Heating Stage, Rotating Monofilament Stage and other accessories

Electron Probe Microanalysis
Energy and Wavelength Dispersive

Transmission Electron Microscopy
Diamond Knife Thin Sectioning of Biological, Polymer, Ceramic and Metallurgical Samples; Replication and Shadowing; Freeze Fracturing and Etching; Stereopairs

Quantitative Image Analysis
"Quantimet" Image Analyzing Computer with Automatic Detector and Shape Discrimination Modules (data taken either from your samples or micrographs)

Auger/ESCA
Complete System Including Ion Gun for Sputter-Etching and Depth Profiling Into the Sample

X-Ray Diffraction
Wide and Small Angle

Optical Microscopy • Thermal Analysis (DTA, TGA, TMA) • Infra-Red Spectroscopy • Particle Size Analysis • Small Particle Identification • Failure Analyses

Expert Consulting—Prompt Results • All services available on short or long term basis
Write or call today for our brochure

STRUCTURE PROBE, INC.
SPECIALISTS IN MATERIALS RESEARCH

Philadelphia
535 East Gay Street, West Chester, PA 19380 • (215) 436-5400

New York Area
230 Forrest Street, Metuchen, NJ 08840 • (201) 549-9350

No matter whose SEM or TEM you choose...

AEI, AMR, ARL, B&L, Cambridge, Cameca, Coates & Welter, ETEC, Hitachi, JEOL, ISI, Leitz, MAC, Perkin-Elmer, Philips, Siemens, or Zeiss.

The best X-ray choice* is the new KEVEX 5100.

Third-generation Kevex 5100 X-ray energy dispersive spectrometers (XES) offer more advantages than any other system for making the most efficient use of your SEM. The key ones are:

1. Highest detector resolution—152 KeV.
2. Highest solid angle with slim 17 mm detector envelope. Snuggle up to the specimen.
3. Rectractable geometry detector.
4. Tailor-made detector/cryostats for every SEM and TEM.
5. Modular analyzer electronics, using plug-in cards and standard NIM modules. Buy what you need, add new capabilities as requirements change.
6. Highest protection against obsolescence. If one component becomes outdated, the rest of the system does not.
7. Color or monochrome video display terminals.
8. MLK marker generator for fast element identification.
9. **Microprocessor** programming for data reduction.
10. Choice of 30 plug-in options for data processing, input-output interfacing, and system customizing.

* The new high-efficiency Kevex Mark IV Detector guarantees 146 eV resolution at 5.9 kev. This new detector features a miniature ½" diameter detector shroud that permits better detector-specimen geometry.

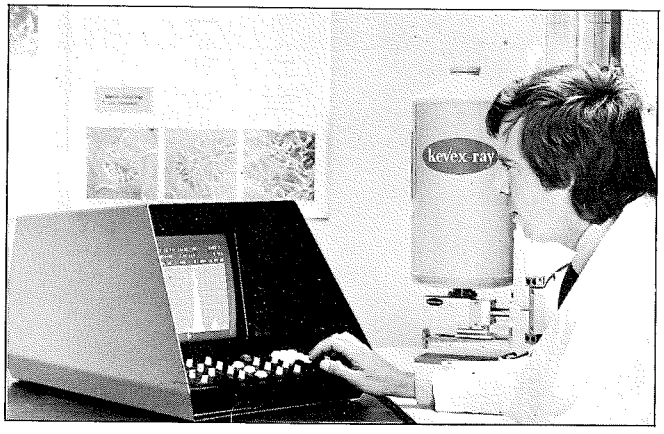

Phone (415) 697-6901 to learn more, or contact us at:

kevex

KEVEX CORPORATION
Analytical Instruments Division
898 Mahler Road • Burlingame, CA 94010
Phone (415) 697-6901

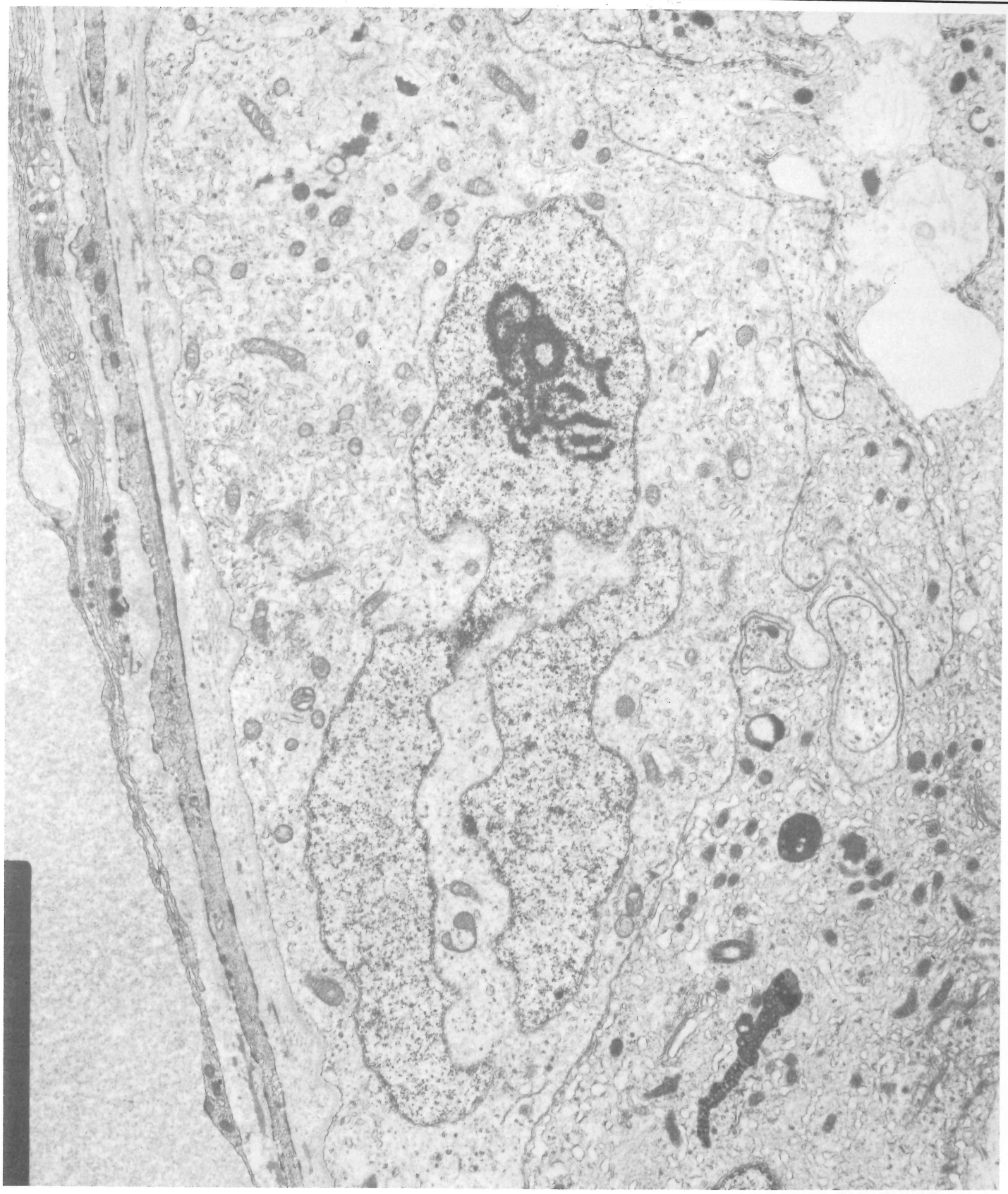

STEM SPERMATOGONIUM OF THE NINE-BANDED ARMADILLO.
Dr. Frank J. Weaker, Department of Anatomy, The University of Texas Health Science Center at San Antonio. This unusually looking cell is believed to be the stem spermatogonium of the nine-banded armadillo. The nucleus is irregular in shape with deep infoldings and frequently displays bizarre configurations. It contains finely packed chromatin granules, which are homogeneously dispersed, as well as one or two prominent nucleoli. The cytoplasm of the stem cell is less opaque than the other germ cells and contains a paucity of organelles with the mitochondria being the most prevalent. Although not shown, the Golgi is usually small and consists of several crescent shaped scaccules and a few small vesicles.

JEOL

JEM-100C

Analytical Electron Microscope

The JEM-100C combines the very best in Transmission (TEM), Scanning (SEM) Scanning Transmission (STEM) & X-ray. The 100C offers the sophistication of four instruments in one plus superior performance in any single mode 3.4A° TEM, 30A° SEM, 15A° STEM, analysis of all elements from sodium on up from microareas of 200 A° or less & selected area diffraction of a 200A° micro-area. Our side entry goniometer provides specimen tilt of ±60° for X axis & 360° rotation or ±45° for X & Y axis. Other accessories now available include a field emission gun & electron energy analyzer.

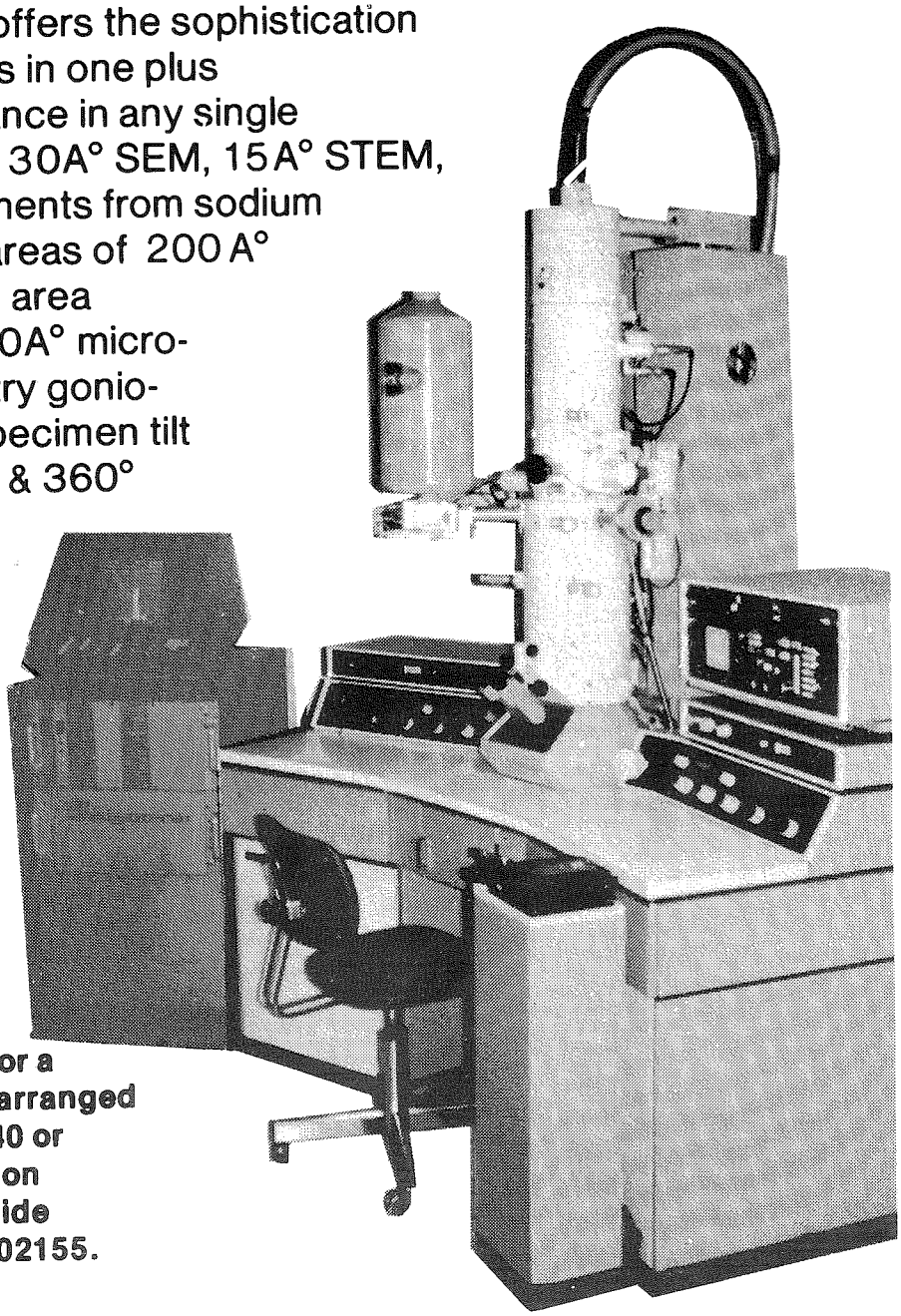

Complete information or a demonstration will be arranged by calling 617/391-7240 or writing JEOL Application Laboratory, 477 Riverside Ave., Medford, Mass. 02155.

Thermionic versus Field Emission ...the future of SEM technology.

Yesterday

When Coates & Welter was formed in 1970 to apply field emission technology to the scanning microscope, SEM performance was limited by the low brightness and energy spread of the thermionic electron gun. When our first CWIKSCAN® SEM's showed a 1000× gain in brightness and an order-of-magnitude reduction in energy spread, most other manufacturers grudgingly began field emission development programs of their own.

Today

Today, you can buy a field emission SEM from Etec, Hitachi, JEOL and most other SEM manufacturers. Because of the substantial performance advantage of field emission over thermionic designs, they've introduced this new technology in "top of the line" premium-cost instruments. At Coates & Welter, we've built only field emission systems for six years. We offer a full range of models from $45,000 . . . and every one of the nearly 200 CWIKSCAN® SEM's in use worldwide incorporates a field emission electron gun.

Coates & Welter's new Model 106A Field Emission Scanning Electron Microscope combines magnifications up to 200,000× (with depth of focus up to 20 times greater than other SEM's) with "matched" electron optics capable of 60Å resolution at 15kv, 300Å at 1kv and 50Å in STEM mode.

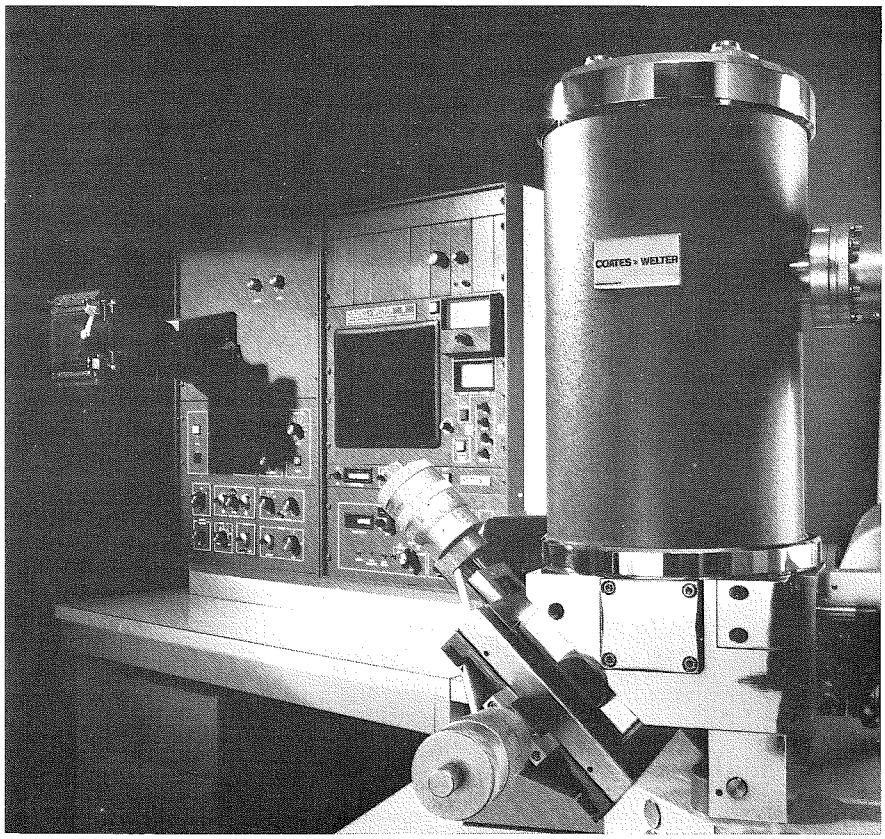

Tomorrow

As other manufacturers learn how to take full advantage of field emission technology, they'll discover exciting new SEM performance features. Eventually, they'll offer flicker-free tv-rate scanning at any magnification *(with a brighter beam, field emission SEM's can scan faster)*. High magnification micrographs of uncoated nonconducting samples with no damage to the sample *(tv scan rates minimize charge effects and sample damage)*. 30Å resolution at high voltage *(some thermionic systems may achieve 60Å)*. 300Å resolution at 1kv *(the best thermionics offer 1000Å at 1kv)*. Greatly reduced maintenance *(contamination-free ion vacuum pumps, no column cleaning, no liner or aperture replacement, for example)*. 20× depth-of-field gain at the push of a button *(like the CWIKSCAN® "lens-off" switch)*. Reduction of typical exposure times from 60 seconds to 16 seconds. Direct video-taping of microphotographic images. Ultra sharp micrographs *(with our unique 4200-line micrographic system)*. And constant, dependable resolution capability because there's no filament deterioration *(there's no filament)*.

Eventually, they'll all develop field emission technology to its full potential. But why wait . . . it's all available today in every Coates & Welter CWIKSCAN® Scanning Electron Microscope.

COATES & WELTER

777 North Pastoria Avenue, Sunnyvale, CA 94086, 408-732-8200

A subsidiary of American Optical Corporation

EM400
Root of castor oil plant.
2 µm thick section.
120kV

To make the invisible more accessible

Philips electron microscopy:

High throughput . . . routine operation (EM201C)	**Multi-parameter analysis . . . practical, comprehensive (EM301C-STREAM)**	**Knowing more about the specimen than ever before . . . exploratory research (EM400) (PSEM500)**

Call George Brock
in our Houston office
713-782-4845

PHILIPS

Abstracts

THE FINE STRUCTURE OF SPERM STORAGE ORGANS OF VIRGIN FIRE ANT QUEENS, T.T. Zboril, Dept. of Life Sciences, Sam Houston State, S.B. Vinson, Dept. Entomology, Texas A&M University.

The gross morphology and ultrastructure of the bursa copulatrix, uterine pouch and spermatheca of **Solenopsis saevissima richteri** Forel were examined using light and electron microscopy. The bursa copulatrix and uterine pouch possessed tubules leading from the secretory epithelial cells to the lumen of the organs. Prominent secretory granules were evident along the base of these cells. Pepsin, Trypsin, and Pronase enzyme digestion resulted in a reduction of electron density of these granules, indicating that these granules contain proteinacious components. Azure II-methylene blue and PAS reactions indicated a concentration of polysaccharides associated with the secretory material within these cells.

ULTRASTRUCTURAL STUDIES OF OUTGROWTH FROM TISSUE EXPLANTS OF HUMAN PROSTATIC NEOPLASIA BY IN SITU EMBEDDING METHOD. Y. Ohtsuki, L. Dmochowski, G. Seman, J.M. Bowen, and D.E. Johnson.* The Univ. of Texas, M.D. Anderson Hospital and Tumor Institute, 6723 Bertner Ave., Houston, Texas 77030.

In order to determine the nature of outgrowing cells from tissue explants, explants of tissues from 2 prostatic carcinoma (PCa) and of a benign prostatic hyperplasia (BPH) obtained by needle biopsy were cultured for 26, 36, and 79 days, respectively. Areas of epithelioid and/or fibroblastic cells were selected under the microscope and fixed **in situ** in 3% glutaraldehyde, and 2% OsO4, followed by embedding in Epon-Araldite. After polymerization, the selected parts were cut out and sectioned either horizontally or vertically. In all cases, free surfaces of explants were covered with one or three layers of epithelial cells showing tonofilaments and desmosomes. These epithelial cells were expanding around the original stromal tissues. Multinucleated giant cells were observed in outgrowth from BPH. No significant ultrastructural differences between epithlial cells from both PCa and BPH were found. In fibroblastic parts of the outgrowth, spindle-shaped fibroblastic cells and smooth muscle cells were proliferating in one or several layers. Thus, it appears that outgrowths from human prostatic neoplasia **in vitro** may contain epithelial cells even after 2 months of cultivation, as demonstrated by electron microscopy. Comparative ultrastructural studies of epithelial cells derived from explants of PCa and BPH may greatly contribute to the analysis of the properties of these cells by other (biological and immunological) methods. Supported in part by Grant CA-15438 from the National Cancer Inst., NIH, USPHS.

DENSITY DEPENDENT G_2 ARREST IN TETRAHYMENA PYRIFORMIS. David W. Heitman, I. L. Cameron and T.B. Pool, Department of Anatomy, The University of Texas Health Science Center at San Antonio, San Antonio, Texas 78284.

DNA synthesis can be synchronized in cultures of the ciliated protozoan **Tetrahymena pyriformis** GL-C by starvation-refeeding. Although most cells are arrested in early G_1, some complete division when refed in the presence of the DNA synthesis inhibitor hydroxyurea. No cells are halted during S phase indicating that a small population of post DNA synthetic (G_2 phase) cells exists following starvation. That these cells are stalled in G_2 with an increase of cell density during starvation. These observations suggest this system to be useful in probing G_2 regulation, therefore, two possibilities are (1) cell mediated chemical modification of the starvation medium, or (2) a cellular collision phenomenon. Small diffusible molecules have been ruled out by a dialysis tubing study. Large diffusible molecules are still a possibility due to the data showing 30% G_2 cells in a population starved at a density of 300,000 cell/ml as compared to 47% G_2 cells at the same density when starved in a dialysis tubing. After starvation a morphological flattening of the cells has been observed. Studies are in progress to further test the density dependent G_2 arrest. Detections of cell cycle dependent morphological changes using SEM and stereo analysis may help identify G_2 cells.

INTERCELLULAR DISTRIBUTION OF ELEMENTS IN MOUSE PANCREATIC ACINAR CELLS BY X-RAY MICROANALYSIS. T.B. Pool, I.L. Cameron, and Nancy Smith, Department of Anatomy, The University of Texas Health Science Center at San Antonio, San Antonio, Texas 78284.

In order to determine the intercellular distribution of elements in a protein secreting tissue, 1mm cubes of pancreas were rapidly excised from Ajax mice and frozen in liquid propane chilled to liquid nitrogen temperature. Sections (4 um) were made at −30° prior to cryosorption at that temperature. To reduce background x-rays, the sections were suspended over a single hole in a copper EM grid using no adhesives and were analyzed at 25 kV in a JEOL JSM-35 SEM equipped with a Nuclear Semiconductor Si (Li) detector. Data were stored and processed with a Tracor Northern NS-880 pulse height analyzer system using appropriate programs and reference standards. Peak to continuum ratios were calculated from characteristic x-rays of Cl, K, P, S and Ca from nuclear, cytoplasmic and zymogen-enriched areas of acinar cells. Although Ca is uniformly distributed throughout the cells, both Cl and S are significantly higher in zymogenic regions as compared to surrounding cytoplasm or nuclei; K and P are significantly lower in zymogenic regions. All elements were seen to be uniformly distributed between nuclei and non-zymogenic areas of the cytoplasm in pancreatic acinar cells.

A NERVE-SPECIFIC SILVER STAINING PROCEDURE FOR STUDY OF INSECT NERVES. Theresa Droste, Entomology Dept., Texas A&M University.

Existing nerve-specific histochemical staining techniques for insects are unreliable in delineating nerves from nonnervous background elements and connective tissue under the SEM. This is due largely to specimen preparation parameters of fixation and heavy metal coating which are standardly employed. A simple, reliable silver staining technique for tracing the innervation of insect internal tissues with SEM was developed, using fresh whole mount dissections staining procedure incorporates three separately-published techniques in which specific aspects of histochemical staining and soft tissue treatment are refined: (A) a tissue pretreatment technique (Herdman and Taylor, 1975) in which the dissected insect heads are fixed in formol-sublimate for a critically-short period of time. This selectively stains nerve fibers, while nontissue impregnation is suppressed. (B) Willard's modifications of Wilder's and Gomori's silver stains

(DeNee, Abraham and Willard, 1974). This simplified technique is applied **en bloc** and the specimens subsequently viewed in the backscattered electron image (BEI) with reversed signal polarity, resulting in an image comparable to silver stained tissue under LM and TEM. (C) An OTOTO method (Kelly, Dekker and Bluemink, 1973) of "coating" the specimens after staining by alternate fixations OsO^4 and thiocarbohydrazide (TCH). This technique is based on the Os-binding properties of TCH, and eliminates the need for heavy metal coating. Combined use of these techniques shows enhanced nerve image contrast from both BEI and X-ray analysis. Problems encountered involve obtaining adequate fixation in the tissue tretreatment to prevent heat-induced image damage to the specimen surface during the silver staining step.

A SYSTEMATIC SEM STUDY OF BACTERIAL CATALYSIS AND THE ACCOMPANYING CORROSION OF THE SULFIDE PHASES IN THE BACTERIAL LEACHING PROCESS. V.K. Berry, Department of Metallurgical and Materials Engineering, New Mexico Institute of Mining and Technology, Socorro, New Mexico 87801.

Thiobacillus ferrooxidans are responsible for catalyzing the oxidation of sulfide minerals to water soluble sulfates in the bacterial leaching process. Direct observation of the corrosion of exposed pyrite (FeS_2) and chalcopyrite ($CuFeS_2$) phase surfaces of a low-grade ore have been made. Energy dispersive X-ray analysis was used in conjunction with scanning electron microscopy to identify sulfide phases. Shake flask technique was employed in this set of experiments. Quantitative data (Cu, Fe^{2+} and Fe^{3+} in solution) were obtained for inoculated flasks and control flasks (uninoculated) at 1 week intervals and bacterial count obtained for inoculated flasks. A marked change in the degree of corrosion in the pyrite and chalocopyrite phases in the inoculated flasks was observed over a period of time with the corresponding increase in the metals(Cu and Fe) solubilized as compared to the control flasks. This change was also accompanied by an increase in the bacterial activity. During the initial periods some selective attachment of the bacteria was observed on the sulfide phases. The attachment was not observed after three weeks' period. This is possibly due to the formation of some surface layer on the sulfide phases as a result of precipitation of iron as hydroxide or as complex jarosite. A comparison of the surface corrosion on pyrite phase surfaces showed some marked differences under identical leaching conditions. This is attributed to the different crystallographic orientations of the exposed crystal surfaces reacting at different rates, since this was the only variable.

SOME COMMENTS REGARDING "PEPPER" IN ELECTRON MICROGRAPHS. Hilton H. Mollenhauer. Veterinary Toxicology and Entomology Research Laboratory, ARS, USDA, P.O. Drawer GE, College Station, Texas 77840.

Thin sections for electron microscopy are often contaminated by extraneous material which appears as electron opaque particles of varying size. Some of these particles arise from reaction of the staining solutions with CO_2 in the air. However, most appear to be dried residues that come from the staining solutions.

There are at least three other kinds of extraneous materials that appear to be in, or on, sections. All of these appear as small dense specks of relatively uniform size distributed over portions of the section. Because of their appearance, these kinds of particles are often called "pepper." The distribution of "pepper" is usually not random and may be heavy over some organelles and absent over others. "Pepper" is most often associated with tissues that are difficult to process such as algae, fungi, and plants.

One kind of "pepper" is due to a vaporization of sectioned material by the electron beam. The other two kinds of "pepper" come about because of (1) an improperly formulated plastic or (2) a reaction between glutaraldehyde and osmium tetroxide during tissue fixation.

All three kinds of "pepper" will be illustrated and methods of preventing them will be discussed.

THE ULTRASTRUCTURE OF HUMAN CHOLANGIOLAR CELLS, Kyung-Whan Min, M.D., Phyllis Gyorkey, M.A. and Ferenc Gyorkey, M.D., V.A. Hospital, Houston, Texas 77211.

The cholangioles are the initial narrow portions of the bile duct to which the bile canaliculi coverage and bile ducts arise. Microscopically, the cells of cholangioles appear intermediary between hepatocytes and ductal epithelial cells exhibiting certain characteristics of both. There are only a few studies of the ultrastructure of the cholagiocholangioles though the liver is one of the organs which has been extensively studied by electron-microscopy.

This report is concerned with the ultrastructure of human cholangiolar cells observed in liver biopsies. The liver tissue was fixed in glutaraldehyde and postfixed in osmic acid and embedded in Epon-Araldite, thin sections were stained with uranyl acetate and lead citrate.

The cholangioles were lined in part by the hepatocytes and by polygonal cholangiolar cells around the luminal space continuous and similar to bile canaliculi. They were attached by desmosomal junctions. The cytoplasmic membrane was smooth except at the luminal borders in which microvilli were present. The cytoplasm matrix near the luminal border was markedly increased in electron density. There was frequent bundles of microfilaments at the periphery. The mitochondria was small and sparse. There were random profiles of rough-surfaced endoplasmic reticulum. Golgi apparatus was rudimentary. Occasional membrane-bound dense bodies were present. Glycogen was absent. The cholangiolar cells have unique cytoarchitecture to suggest certain specific function(s), such as active bile transport.

AN ULTRASTRUCTURAL STUDY OF RAT AORTIC ARCH BARORECEPTORS. J.M. Krauhs, P.S. Baur and J.L. Long. Department of Physiology and Biophysics, University of Texas Medical Branch, Galveston, Texas 77550.

Fibers of the left aortic depressor nerve of the rat respond to pressure stimuli applied to the aortic arch and play a role in the control of blood pressure. Methylene blue was used to stain aortic nerve-arch preparations which were then observed as whole mounts in order to trace the course of the fiber bundles. Dorsal and ventral branches of the nerve innervate the tunica adventitia of the aortic arch between the left common carotid and left subclavian arteries. Pressure on the region innervated by the ventral branch stimulates firing in the aortic nerve (W. R. Saum, personal communication); therefore, this area was chosen for ultrastructural studies. The aortic nerve branches were composed of myelinated and unmyelinated fibers. In the outer adventitia, these usually occurred together in small bundles 2 - 18 μm in diameter. At deeper levels, bundles were no longer recognizable as such and the myelinated fibers had lost their myelin. Irregularly-shaped fiber profiles containing large numbers of mitochondria and glycogen granules were observed along with the smaller unmyelinated fibers with few mitochondria. Sometimes clear vesicles about 40 nm in diameter were also present in the mitochondria-filled fibers. More distal regions of these fibers were only partially covered by Schwann cells. The rest of the plasma membrane was directly exposed to the extracellular connective tissue matrix and appeared to be

coupled to basal laminae by means of electron-dense "bridges." No differences between normal and spontaneously hypertensive rat baroreceptors were observed. Supported by NIH grant H. -19048.

COLONIZATION OF THE GASTROINTESTINAL TRACT OF MICE BY CANDIDA ALBICANS: A MODEL SYSTEM FOR EXAMINATION OF HOST-PATHOGEN RELATIONS DURING DEVELOPMENT OF INTESTINAL CANDIDIASIS. Garry T. Cole[1], Leanne Field[2] and L. Joe Berry[2], Departments of Botany[1] and Microbiology[2], University of Texas at Austin.

Candida albicans is a common component of the microflora found in the human intestinal tract. In a healthy individual, the yeast does not establish infectious colonies. However, if broad spectrum antibiotics are administered to an individual for long periods, the competition between the fungus and bacteria is reduced and the chances of contracting intestinal candidiasis are increased. This problem is even more acute for patients who are subjected to immunodepressant drugs, such as those employed in cancer chemotherapy. Little is known about the pathogenicity of **C. albicans.** In our initial studies of intestinal candidiasis, which have involved use of orally infected laboratory mice, we have been mainly concerned with the establishment of an experimental model for testing various aspects of host-pathogen relations. Because of the high motility in the gut of mice, colonization by **C. albicans** usually does not occur but was enhanced in our system by oral administration of tobramycin and ip injections of lomotil. The extent of colonization was monitored by excising and homogenizing organs of the gastrointestinal tract which were subsequently plated out in a dilution series on Sabourauds dextrose agar. The ultrastructural features of infected tissues were examined in the SEM. In this report, we demonstrate the structural association between yeast cells and different parts of the intestinal tract 2-4 weeks after oral challenge and discuss the possible mechanisms of adherence for the pathogen and to host tissue. The results of these studies provide the basis for continued investigation of the process of penetration of the epithelial mucosa during early stages of systemic infection by **C. albicans.**

THE MORPHOLOGY AND PROPOSED FUNCTION OF TWO DOME-SHAPED SENSILLA ON THE OVIPOSITOR OF THE INSECT PARASITE Cardiochiles nigriceps. Margaret R. Barlin, Department of Entomology, Texas A&M University.

The behavior and physiology of hymenopterous parasites are finely attuned to that of their hosts. Two important stages in successful parasitization are host finding and host acceptance. If these stages are examined closely, the major fundamental components are recognized as mechanoreception and chemoreception. The ovipositors of **C. nigriceps** females play an important role in detecting the insect host and in discrimination of a viable host, both before and after ovipositor insertion. The ovipositor consists of a pair of fused second valvulae and a pair of first valvulae. Scanning electron micrographs show two types of dome-shaped sensory sensilla, each located in a depression in the cuticle. The sensilla are concentrated on the fused second valvulae with both types occurring on the distal tip; the first type, which appears to have a mechanoreceptor function, is more numerous than the second type, which probably functions as a chemoreceptor as it has a pore at its apex. The first type also occurs down the length of the ovipositor in relatively straight rows. The first valvulae have distal barbs, immediately proximal to each of which is a chemoreceptor-type sensillum. The function of these sensory receptors was investigated further with transmission electron microscopy. It is thus evident that the ovipositor of this parasite has evolved into an efficient organ to detect environmental stimuli essential for the survival and success of the species.

ULTRACYTOCHEMICAL LOCALIZATION OF THE NA+K - ACTIVATED ADENOSINE-TRIPHOSPHATASE IN THE BRANCHIAL EPITHELIUM OF A EURYHALINE TELEOST. Seth R. Hootman and Charles W. Philpott, Department of Biology, Rice University, Houston, Texas 77001.

The activity of the electrolyte transport enzyme, Na+K - activated adenosinetriphosphatase, in gill homogenates from the euryhaline teleost **Lagodon rhomboides** increases to over 200% of its previous value following transfer of these fish from brackish water to artificial seawater. In order to assess the cellular events which accompany this increase, we have utilized an ultracytochemical method based upon the potassium-dependent phosphatase activity of the enzyme to visualize sites of Na+K−ATPase activity in the branchial epithelium.

The heaviest depositions of reaction precipitates were confined to "chloride cells," although staining was observed along the plasma membranes of most cells in the epithelium. The labyrinth of anastomosing plasma membrane tubules which ramify throughout the cytoplasm of the chloride cells was heavily stained, with granular precipitates lining the cytoplasmic membrane surfaces. Enzyme activity was also noted on the apical crypt membrane, on membranes of vesicles in the cytoplasm subjacent to the crypt, and on Golgi membranes of visicles in the cytoplasm subjacent to the crypt, and on Golgi membranes. Stain deposition was much reduced by deletion of potassium or inclusion of ouabain in the incubation medium, thereby validating the assumption that the observed precipitates represent sites of Na+K−ATPase activity. Supported by NSF grant P4B3634.

THE EFFECT OF THE SOURCE OF CHLORIDE ION ON THE COPPER-ALUMINUM CEMENTATION RATES: A SCANNING ELECTRON MICROSCOPIC STUDY. Velu Annamalai, Department of Metallurgical and Materials Engineering, New Mexico Institute of Mining and Technology, Socorro, New Mexico 87801.

Commercial recovery of copper from pregnant leach liquors is carried out utilizing the cementation technique of depositing metallic copper on scrap-iron. The drawback of the process is, however, the excess consumption of iron; some plants have as high as 260%. Aluminum in the form of beverage and beer cans due to its abundant availability has been tried as an alternative to scrap-iron to cement copper. The usage of aluminum in the process would seem to help solve the ecological problem of can-littering, in addition to the economical utilization of waste-cans as compared with the cost of energy required in reclaiming the aluminum metal.

Any freshly produced aluminum surface will react instantly with oxygen to form a thin but tight, non-porous and protective oxide layer. No cementation will take place unless the oxide layer is removed. Earlier studies showed that chloride ion (>15ppm) is effective in destroying the layer. Also, the reaction rates seemed to depend on the structure and morphology of the resultant deposits when any experimental parameter was varied. A cementation cell in conjunction with pure aluminum (99.99%) rotating discs was used in these studies. The present report highlights the change in the cementation rates with different sources of chloride ion, such as KCl, NaCl, $AlCl_3$, Hcl, etc. Further, the observation of the structural characteristics of the deposits by scanning electron microscope has provided a direct physical evidence to the change in the rates. Corrosion patterns under these conditions have also been studied and correlated to the total aluminum consumed in the system.

X-RAY MICROANALYSIS OF THE NUCLEAR-CYTOPLASMIC DISTRIBUTION OF ELEMENTS IN MOUSE HEPATOCYTES. Rodney L. Sparks and Nancy R. Smith, Department of Anatomy, The University of Texas Health Science Center at San Antonio, San Antonio, Texas 78284.

The mechanisms of control of cellular processes can be better understood with a knowledge of the concentration and distribution of elements at the subcellular level. Unfixed frozen-dried 4 micron sections were used. The sections were examined at 25 kV in a JEOL JSM-35 scanning electron microscope equipped with a Nuclear Semiconductor Si (Li) detector. The data were collected, stored and processed by a Tracor Northern NS-880 pulse height analysis system using the Flexatran Super Multiple Least (ML) Squares fitted algorithm program and appropriate elemental reference standards. Elemental distributions were determined by using peak/continuum ratios between nucleus and cytoplasm of 5 hepatocytes. Continuum gives a measure of mass and shows that the nucleus has 28% less mass than cytoplasm ($p < .05$). The nuclear-cytoplasmic ratios (n/c) were calculated for each cell and statistically analyzed. The five detectable elements of biological relevance and their n/c ratios are : Na(1.27), P(1.12), S(1.10), K(1.08) and C1(0.88). A ratio greater than one indicates higher concentration in the nucleus. The ratio of C1 was shown to be significantly less than the ratios of all the other elements and the ratio of K was significantly less than Na. These data show that elements are differentially partitioned between nucleus and cytoplasm.

CELL-CYCLE KINETIC AND ULTRASTRUCTURAL ANALYSIS OF ASYNCHRONOUS X-IRRADIATED CHINESE HAMSTER CELLS: A FLOW MICROFLUOROMETRIC-QUANTITATIVE ELECTRON MICROSCOPIC STUDY. S.S. Barham, D.E. Swartzendruber, and R.A. Walters, Cellular and Molecular Biology Group. Los Alamos Scientific Laboratory, University of California, Los Alamos, New Mexico 87545.

A bromodeoxyuridine (BUdR)-mithramycin technique for detecting noncycling and slowly cycling cells in proliferating populations has been applied to Chinese hamster (line CHO) cells irradiated in suspension culture with 800 or 1200 rad. This technique can differentiate among cells that have either not replicated their DNA, replicated once, or replicated two or more times. Flow microfluorometric (FMF) analysis of irradiated cells subsequently grown in the presence of BUdR indicates that each cell may divide once but only once after radiation exposure. Cell counts and mitotic fractions scored from samples fixed at regular intervals post-irradiation support the FMF data. Profiles of cells in thin section were scored by transmission electron microscopy at regular intervals post-irradiation for the presence of visible nuclear lesions. Quantitative microscopic data indicate that visible lesions within the cell nucleus do not appear until cell division has occurred post-irradiation. Visible intranuclear damage was not observed during the 8 to 12 hr division delay period induced by 800 or 1200 rad. Increasingly greater fractions of cells in irradiated populations displayed nuclear damage from the end of the division delay period up to 72 hr post-irradiation, suggesting that radiation effects leading to visible morphological changes are cumulative. The results indicate that nuclear lesions are morphologically expressed only after cells have passed through one chromatin condensation-decondensation cycle (i.e., mitosis). (This work was performed under the auspices of the U.S. Energy Research and Development Administration.)

ULTRASTRUCTURE OF BASIDIOSPORES AND BASIDIOSPORE GERMINATION IN THE RUST FUNGUS GYMNOSPORANGIUM JUNIPERI-VIRGINIANAE. Charles W. Mims, Department of Biology, Stephen F. Austin State University, Nacogdoches, Texas 75962.

Basidiospores of **G. juniperi-virginianae** are typically pear shaped and measure about $17\mu m \times 10\mu m$. Each spore contains many ribosomes as well as lipid droplets, mitochondria, small vesicles, endoplasmic reticulum and structures thought to be microbodies. Mature spores are either uninucleate or binucleate although larger, tetranucleate spores were occassionally observed. A conspicuous spindle pole body is associated with each nucleus. The spore wall appears as a thin layer except around the hilar region where two layers are evident. Germination is almost always lateral although no germ pore region was noted in the wall. Vacuolation takes place during germination and lipid bodies disappear. The wall of the germ tube arising from the spore is continuous with that of the spore. In some instances a smaller, secondary spore is formed at the tip of the germ tube emerging from the basidiospore.

TRANSFORMATION OF CHICK CHORIOALLANTOIC MEMBRANE BY ROUS SARCOMA VIRUS: IN VIVO AND IN VITRO COMPARISONS. Susan L. Fullilove, Cell Research Institute, University of Texas at Austin, Austin, Texas 78712.

The morphology of the chick chorioallantoic membrane (CAM) 3-4 days after infection with Bryan high-titer strain of Rous sarcoma virus was compared with that of pieces of CAM infected **in vitro** and cultured for similar periods of time. At the light microscope level the appearance of the three layers of the CAM (chorionic, mesodermal, and allantoic) in culture was similar to the CAM transformed **in vivo** except that hyperplasia of the two epithelial layers rarely occured **in vitro.** Ultrastructurally the **in vitro** CAMs compared well with the tissue **in vivo** also. Since the purpose of this study was to establish the feasibility of culturing pieces of CAM for continuing investigations into the cellular events and biosynthetic aberrations associated with transformation, with particular emphasis on changes in matrix composition, several observations pertinent to these subjects are also reported. (Supported by NIH Training Grant CA 09182)

RADIOAUTOGRAPHIC STUDIES OF FRIEND LEUKEMIA VIRUS-CONTAINING MURINE CELLS Claire E. Hulsebosch, Cell Research Institute, University of Texas at Austin, Austin, Texas 78712

Friend leukemia virus transformed cells (FSD-1/clone 4), stimulated with dimethyl sulfoxide to promote erythroid differentiation, were incubated at 37°C for 30 minutes in either L-Fucose-1-H^3 or D-Galactose-1-H^3 with chase intervals ranging up to 2 hours. Samples of cells were fixed in glutaraldehyde and embedded in Epon-Araldite using conventional electron microscopy techniques. Sections of embedded material 1 μ thick were used in light microscope radioautographic studies as an index for exposure time for electron for the light microscope radioautographs, it was clear that true electron microscope radioautography would not be adequate as a research tool. Both fading of latent image and breakdown of specimens would occur over the time required to achieve a usable amplitude of labeling if thin sections of material were used. For this reason, sections $1/4\mu$ thick were used for intermediate resolution electron microscope radioautography. This technique and the results obtained will be discussed.

CELLULAR LOCATION OF COLON TUMOR ASSOCIATED PROTEINS Cameron E. McCoy, Wm.B. McCombs, Nancy D. Mabry and A. Leibovitz.

Proteins produced by colon tumor cells and released into the growth medium were concentrated by membrane sieving and injected into rabbits. The immunoglobulin fraction of the

ORTEC

Materials Analysis Division

5200 M Economy Energy Dispersive System

The New Low-Cost Microanalysis System for All Scanning and Transmission Electron Microscopes

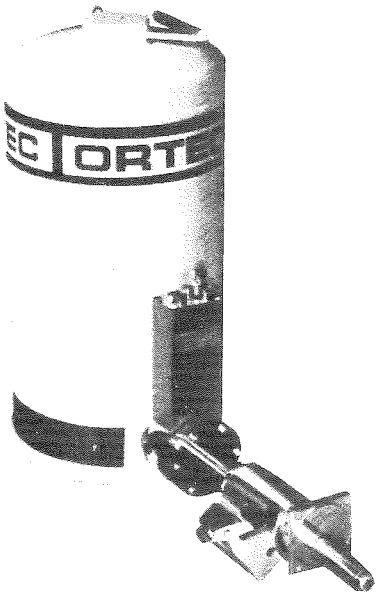

The 5200M Economy Energy Dispersive System from ORTEC offers all necessary functions and many additional features not present on more expensive systems. With its low price, the 5200M is particularly suitable for the modern low-cost Scanning and Transmission Electron Microscopes.

Even the Most Basic 5200M System Offers the Following Features:

Detector
- Premium resolution
- Dynamic charge restoration preamplifier
- Exclusive detector collimation arrangement
- Adjustable detector-to-specimen distance
- Large 7.5-liter dewar

Electronics
- Easily updateable NIM bin and electronics
- Pulse-Pileup and live-time correction
- 3000 V detector bias power supply

Options Available
- Unique Telescoping Interface
- Liquid Nitrogen Level Monitor
- Log/Linear Audio Ratemeter
- KLM Marker
- Camera
- X-Y Plotter

Multichannel Analyzer
- Low dead-time CRT display
- Direct energy readout
- Cursor analog control
- 1024-channel memory
- Compares two spectra
- Region-of-interest integration
- 99,999,999 maximum integral
- 1 million counts full scale
- 0-10, 0-20, 0-40 energy ranges
- Horizontal expand and roll capability
- Add or subtract data
- Erase time and/or memory
- Dead-time meter
- Digital line scan
- X-Y Plotter Interface
- Vertical expansion

antiserum was isolated and used to identify the tumor associated proteins which were antigenic. Separation and characterization of the tumor protein pool was accomplished by isoelectric focusing. Proteins with a given isoelectric point were pooled and tested against each antiserum using Ouchterlony double diffusion and electrophoretic methods.

Carcinoembryonic Antigen (CEA) known to be associated with the colon tumor cells was recognized by the antisera in addition to several other proteins. as determined by comparison with a known antiserum.

Fluorescent antibody and immunoperoxidase techniques were used to determine the cellular location of these tumor associated proteins. As previously reported. antiserum containing anti-CEA caused a positive fluorescence localized to the plasma membrane. Immunoelectron microscopy confirmed the cell surface localization of a protein but also revealed a cytoplasmic protein that was recognized by the antiserum.

PHYSIOLOGICAL CASTRATION IN FEMALE RATS BY ALPHA FETOPROTEIN FROM A HEPOTOMA. T.B. Pool, N. Hagino and I.L. Cameron, Department of Anatomy, The University of Texas Health Science Center at San Antonio, San Antonio, Texas 78284.

We have studied the reproductive biology of female Buffalo rats bearing Morris hepatoma #7777. Electrophoretic patterns of serum proteins from control and tumor bearing rats were compared by integrating peak areas from densitometer tracings. Two peaks, present only in sera from hepatoma-bearing rats, co-migrate with slow and fast alpha fetoprotein (AFP) from rat amniotic fluid. As tumor size increases, these two peaks increase in area whereas that of another serum protein (albumin) decreases. Vaginal smears are prepared daily from control and tumor-bearing rats. Hepatoma-bearing females remain in diestrus once the tumor exceeds a cross sectional area of 12 cm^2. The ovaries from these rats have enlarged sinusoidal-like capillaries surrounding the luteal cells. The epithelium of the uterine mucosa is thinner and less vacuolated in tumor-bearing females than in controls; this is also correlated with a significant decrease in uterine wet weight in tumorous rats as compared to controls. Pituitary gonadotrophic cells in hepatoma-bearing rats are enlarged and possess an ultrastructure similar to gonadotrophic cells from ovariec-tomized rats (castration cells). Serum estrogen levels, as determined by radioimmunoassay, were elevated 3 to 23 fold in tumor-bearing animals over control values, with the higher levels corresponding to females with larger hepatomas. Rat AFP can bind estrogen and we conclude that the elevated levels of AFP in sera of hepatoma-bearing rats are responsible for the changes in reproductive biology we have seen. Presumably, estrogen bound to AFP is unable to exert normal physiological action.

ULTRASTRUCTURAL LABELING OF CELL SURFACE LECTIN RECEPTORS IN THE CHANG RAT HEPATOMA, Peter C. Moller, Ph.D., Jeffrey P. Chang, Ph.D., Division of Cell Biology, University of Texas Medical Branch, Galveston, Texas 77550.

The mobility of concanavalin A (Con A) surface receptors in the solid & ascites tumor form of the Chang rat hepatoma growing under **in vivo** & **in vitro** conditions were investigated cytochemically. The cells were incubated in Con A & horseradish peroxidase (PO), either with or without prior glutaraldehude fixation, and subsequently treated with DAB.

In cells fixed before Con-A-PO labeling the reaction product was localized as a continuous layer upon the external surface of the plasma membrane. If unfixed cells were treated with Con A and coupled with PO at 4°C and reincubated in PBS at 37°C for varying periods of time, the labeling pattern was discontinuous. Some portions of the plasma membrane were devoid of label and after 60 minutes of reincubation in warm PBS, the cell surface was almost completely free of Con-A-PO reaction product. In as little as 15 minutes of reincubation endocytotic vesicles and multivesecular bodies containing PO positive material began to appear within the cytoplasm and in some instances, in close proximity to the Golgi apparatus. No differences in surface labeled material could be detected between solid tumor or ascites cells or between cultured and **in vivo** material. Pretreatment of cells with α-methyl-D-mannoside before lectin labeling resulted in non Con-A-PO label being formed. The data shows that lectins can induce internalization and redistribution of plasma membrane and is time and temperature dependent. (Supported by a NIH research grant CA 16663 from U.S.P.H.S.).

INTRACELLULAR SYNTHESIS PATHWAYS OF SECRETORY PROTEINS, Jeffrey P. Chang, Ph.D., Division of Cell Biology, University of Texas Medical Branch, Galveston, Texas 77550.

It has been established (Palade, Science 189:347, 1975) that the intracellular synthetic and secretory pathways of the digestive secretory proteins in pancreatic or intestinal epithelial cells include (1) synthesis of polysomes attached to ER, (2) segregation in the cisternal space of RER, (3) transport to the Golgi, (4) concentration by condensing granules, (5) intracellular storage, and (6) discharge by exocytosis. Recent results from our laboratory indicated that the synthetic pathway of the secretory protein, albumin, does not follow those for digestive secretory proteins.

Rat albumin was injected to rabbit to produce Fab fragment of IgG for conjugation with horseradish peroxidase. This conjugate was incubated with tissue sections plus 3, 3'-diaminobenzidine to localize the sites of albumin synthesis under electron microscope. In rat liver, kidney, aorta and the Chang hepatoma, the most intense reaction product appeared on polysomes attached to ER or nuclear envelope. Albumin molecules have never been observed in the cisternal spaces of any cytomembranes. Therefore, the albumin protein appears being synthesized by polysomes bound to ER or nuclear envelope and discharged directly into cytosol for secretion into extracellular spaces. (Supported by a NIH research grant Ca 16663 from U.S.P.H.S.).

THE ULTRASTRUCTURE OF MESOTHELIAL CELLS IN BODY FLUIDS. Kyung-Whan Min, M.D., Phyllis Gyorkey, M.A. and Ferenc Gyorkey, M.D. V.A. Hospital, Houston, Texas 77211.

The mesothelial cells lining the body cavities undergo reactive changes and these atypical cells shed into the effusions. The diagnosis of the cells in the body fluids are often difficult to differentiate from truly malignant cells.

We have studied 46 body fluids with neoplastic cells or with highly atypical cells suspicious for malignancy and characterized the fine structural features of the atypical mesothelial cells.

The cell nuclei were usually round with peripherally dispersed chromatin and one or more nucleoli. The nuclear-cytoplasmic ratio varied and corresponded with the degree of atypicality. The cytoplasmic features were unique. There were profiles of regularly spaced rough-surfaced endoplasmic reticulum (RER) dividing the cytoplasm in zones. The cytoplasmic matrix between RER were fibrillar and contained few mitochondria and scattered polysomes. Frequently the fibrillar cytoplasmic matrix formed stacks of microfilaments. The cytoplasmic borders were usually smooth and microvilli were present in less than one-third of cells. Another feature was the presence of glycogen in large aggregates near the periphery. The

mesothelial cells were usually seen singly.

Our study indicated that electron microscopy is a useful tool to differentiate atypical mesothelial cells from other neoplastic cells in the diagnosis of body fluids.

NEUROSARCOMA, Bruce Mackay, M.D. Anderson Hospital, Houston.

Benign tumors of the peripheral nervous system (schwannoma, neurofibroma) are common, and they can usually be classified by light microscopy. In contrast, criteria for the diagnosis of malignant peripheral nerve tumors are limited. Neurosarcoma will be suspected when malignant transformation occurs in a schwannoma or neurofibroma, or if a patient with neurofibromatosis develops a sarcoma; but the identification of these tumors from their appearance in light microscopic sections is often difficult and may be impossible. The ultrastructural features of the benign peripheral nerve tumors are distinctive, and they are to varying degrees recapitulated in the malignant nerve sheath neoplasms. By using electron microscopy, it is consequently possible to recognize most neurosarcomas, and we have now studied a large enough number of cases to be aware of the range of fine structure that may be encountered in these tumors. In turn, this information is revealing that neurosarcomas possess a hitherto unsuspected spectrum of light microscopic histology. Our ability to identify neurosarcomas is opening the way to studies of the biologic behavior of these tumors, and will permit assessments of their response to various forms of therapy.

ULTRASTRUCTURAL FEATURES OF SESICCATED EMBRYONIC BEAN ROOT TIP USING A NON-AQUEOUS FIXATION TECHNIQUE. Betty Hamilton and Glenn Todd, School of Biological Sciences, Oklahoma State University, Stillwater, OK 74074.

The development of most angiosperm seeds includes a period of dormancy during which the water content of the tissue falls to ca. 15% or less. Such tissues are metabolically inactive, show remarkable resistance to various types of environmental stress and resume active metabolism immediately upon imbibition of water. Such tissues must reflect both the metabolic inactivity and the potential for rapid resumption of metabolism in their ultrastructure. Convential fixation procedures were found to be unsatisfactory because hydration of biopolymers occured during the fixation steps. This resulted in major changes in cellular morphology and specimens which did not represent the structural state of dormant, disiccated tussue. An alternative procedure using dimethylsulfoxide (DMSO) to carry dried glutaraldehyde and chloroform to carry OsO^4 avoided many of the artifacts seen in more conventional preparations.

Most observations are of cortical parenchyma ca. 1-2mm from the extreme root tip of dormant **Phaseolus vulgaris** L. embryos. The most striking feature of the tissue is the contorted, compacted aspect. Cell walls are folded, with closely appressed cytoplasm. Lipid droplets are abundant at the cell periphery. Protein bodies are numerous, with a granular matrix, and are often decorated with arrays of ribosomes. The nucleus is prominent with distinct nucleolus and heterochromatin, and plastids are recognizable due to the presence of phytoferritin and small starch granules. Free ribosomes fill all otherwise unoccupied space in the cytoplasm. Mitochondria are difficult to recognize.

MYOFIBROBLAST ANCHORING SUBSTANCE (MAS). P.S. Baur, Ph.D., G.F. Barratt, M.S., and D.L. Larson, M.D., University of Texas Medical Branch, Galveston, Texas 77550, Shriners Burns Institute, Galveston, Texas 77550.

Contractile fibroblasts (myofibroblasts) are major cellular constituents of clinically active hypertrophic scars and scar contractures resulting from thermal insult. These cells appear to be implicated in the formation of these wound healing tissues. The premise that myofibroblast contractibility alone can account for the aberrant microarchitecture of these tissues is valid only if the cells are firmly attached to each other and the juxtaposed connective tissue (collagen fibers).

A proteinecious fibrillar material has been routinely observed on the external surfaces of the myofibroblasts when scar tissues are examined by means of transmission electron microscopy. This material, tentatively called the myofibroblast anchoring substance (MAS), appears to firmly attach cells to cells or cells to adjacent collagen fibers. The MAS attachment sites appear to be relegated, for the most part, to those areas of the plasma membrane which overlie the terminations of the contractile bundles (actin filaments) found within the cytoplasm of the myofibroblasts. A more detailed elaboration of the fine structure of this substance and its role in scar contractibility will be similarly discussed.

Regional News

DALLAS: UT Southwestern Medical School.

Notification of Grant Award: Dr. Jerry Shay, Dept. of Cell Biology, N.I.H. "Analysis of Heart Cell Contraction."

E.M. Education: Currently eight students are enrolled in the graduate level "Cell Fine Structure" course offered by Dr's Peter Andrews and Jerry Shay.

LUBBOCK: Texas Tech University, Department of Biological Sciences.

Publications: Smutzer, G. and J.D. Berlin. 1976. The use of Nomarski interference contrast microscopy as an alternative to the staining of Epon sections following autoradiography. Trans. Amer. Micro. Soc. 95: 109-112.

Ramsey, J.C. and J.D. Berlin. 1976. Ultrastructure of early stages of cotton fiber differentiation. Botanical Gazette 137:11-19.

Burbano, J.L., T.D. Pizzolato, P.R. Morey, and J.D. Berlin. 1976. An application of the Prussian blue technique to a light microscope study of water movement in transpiring leaves of cotton **(Gossypium hirsutum** L.). J. Exptl. Botany 27:134-144.

Pizzolato, T.D., J.L. Burbano, J.D. Berlin, P.R. Morey, and R.W. Pease. 1976. An electron microscope study of the path of water movement in transpiring leaves of cotton **(Gossypium hirsutum** L.). J. Exptl. Botany 27:145-161.

Barham, S.S., J.D. Berlin, and R.B. Brackeen. 1976. The fine structural localization of testicular phosphatases in man: The control testis. Cell Tissue Res. 166:497-510.

Ramsey, J.C. and J.D. Berlin. 1976 Ultrastructural aspects of

early stages in cotton fiber elongation. Amer. J. Botany 63:868-876.

Berlin, J.D. and G. Smutzer. 1976. An autoradiographic study of the outer epidermis of the cotton ovule. Beltwide Cotton Production Research Conferences, Proceedings. In Press.

Smith, F.E. and J.D. Berlin. 1976. Cytoplasmic annulate lamellae in human spermatogenesis. Cell Tiss. Res. 176:235-242.

News Briefs: Fannie Smith, TSEM Student Representative for 1975-76, successfully defended her dissertation entitled "Human Spermatogenesis: A study of the Spermatogonial Population and Ultrastructural Aspects of Spermatozoal Development" November 30, 1976, Fannie has accepted a Postdoctorate with Dr. I.B. Fritz, Department of Medical Research, Banting and Best Institute, Toronto, Canada.

Meetings: Dr. Jerry Berlin was the Program Chairman for the Cotton Physiology Group at the Beltwide Cotton Production Research Conferences held in Atlanta, Georgia during January 1977. In addition to 35 contributed papers the program consisted of a symposium entitled "Physiological Research in Cotton Germplasm" with eight presentations.

TEMPLE: Scott & White Clinic, Department of Microbiology.

Meetings: Albert Leibovitz attended the 30th Annual Symposium on Fundamental Cancer Research at the University of Texas System Cancer System in Houston Mar. 1-4 and the meeting of the Texas Branch Society of American Society of Microbiology.

Dr. Wm. B. McCombs attended an ASCP workshop in Chicago, Ill. entitled Advanced Microbiology: Recent Advances and New Frontiers. He was also present for the ASCP-CAP National Convention in Miami Beach, Florida.

DENTON:Texas Woman's University, Department of Biology.

Publications: P.C. Schroeder and Paula Pendergrass. The inhibition of in-vitro ovulation from follicles of the teleost, **Oryzias latipes,** by cytochalasin B.J. Reprod. Fert. (1976) **48,** 327-330.

EM Courses: Techniques in Electron Microscopy will be offered by Dr. Pendergrass in the Fall of 1977.

COLLEGE STATION: Texas A&M

Grants Awarded: Michael Taranto and Dr. K. Mattil, director of Food Protein Research and Development Center at Texas A&M University have been awarded a grant from NSF. The title of their research project is "Physio-chemical Properties of Texturized Protein Products." Funding totaled $59,145.

Lectures: Dr. Jo Ann Shively, Department of Veterinary Anatomy, TAMU, presented a paper entitled "A Method for Evaluation of Bone Ingrowth into Implanted Porous Biomaterials" at the Veterinary Orthopedic Society in Vail, Colorado on February 21, 1977.

Dr. E.L. Thurston, TAMU Electron Microscopy Center, presented programs in scanning electron microscopy to General Dynamics Corp., Dallas, TX, February, 16-18, and to the Veterinary School at Oklahoma State University, February 22-23, 1977. Other presentations by Dr. Thurston included "Microscopy and Molecular Assembly" at the Annual Science Symposium, Austin, TX, February, 26th and "What Ever Happened to Bobby Hooke?" to the Tri Beta Society on April 14-16, 1977.

Dr. Thurston also attended the EMSA Executive Council Meeting in association with Northern California Society for Electron Microscopy in San Francisco, CA on February 9, 1977.

Those attending IITRI-SEM/1977 from TAMU included **E.L. Thurston, A.E. Sowers,** and **J.A. Shively.** Mr. Sowers presented a paper entitled "Growth in Living Plants after Repeated Direct Examination by SEM."

HOUSTON: Baylor College of Medicine, Department of Neurology

Presentations: Dr. Ronald F. Dodson presented Ultrastructural Changes Following Experimental Cerebral Ischemia in the Gerbil in the Neuropathology Section of the Sixth Annual Meeting of Neurological Science in Toronto, Canada, November 7-11, 1976. Coauthors were K.M.A. Welch and L. W.-F. Chu.

Publications: Dodson, R.F., Tagashira, Y., Chu, L.W.-F.: Acute ultrastructural changes in middle cerebral artery following mechanical injury and ischemica produced by surgical clamping. Canad. J. Neurol. Sci. 3:23-27, 1976.

Meyer, J.S., Welch, K.M.A., Titus, J.L., Suzuki, M., Kim, H.S., Perez, F.I., Mathew, N.T., Gedye, J.L., Hrastnik, R., Miyakawa, Y., Achar, V.S., Dodson, R.F.: Neurotransmitter failure in cerebral infarction and dementia. Neurobiology of Aging, Edited by Robert D. Terry and Samuel Gershon, pp. 121-138.

Dodson, R.F., Tagashira, Y., and Chu, L.W.-F: Acute pericytic response to cerebral ischemia. J. Neurol. Sci. 29:9-16, 1976.

Dodson. R.F., Patten, B.M., Hyman, B.H., and Chu, L.W.-F.: Mitochondrial abnormalities in progressive ophthalmoplegia. Cytobios. 15:57-60, 1976.

SAN ANTONIO: Southwest Research Institute.

Presentations: Davidson, D.L., and Laukford, J. 1977. Environmental alteration of fatique crack tip plasticity as determined by electron channeling. Presented at the National Association of Corrosion Engineers Research Conference, San Francisco, March 1977.

Davidson, D.L. 1977. The use of channeling contrast in the study of material deformation. Presented at the Scanning Electron Microscopy Symposium, Chicago, March 1977.

News Briefs: Dr. David L. Davidson has been promoted to Staff Scientist.

The SEM Fatique stage being designed is now operational. It is capable of applying up to 1,100 lbs. load; it is electrohydraulic, therefore, load interaction studies on crack propagation (i.e., overloads) may be investigated, as may crack initiation. The specimen may be observed by both secondary and backscattered electron emission.

The University of Texas Health Science Center at San Antonio, Department of Anatomy.

Grants Awarded: Smith, Nancy, and Sparks, R. "Study of elemental distribution in normal vs. transformed hepatocytes." Institutional Research Grant.

Articles: Cameron, I.L., W.J. Ackley, and W. Rogers. 1977. Responses of hepatoma bearing rats to total parenteral hyperalimentation and to **ad libitum** feeding. J. Surgical Res., (in press).

Cameron, I. L., R.L. Sparks, K.L. Horn, and N.R. Smith. 1977. Concentration of elements in mitotic chromatin as measured by X-ray microanalysis. J. Cell Biol., (in press).

Carter, J.W., and I.L. Cameron. 1977. Sublethal effects of a pure polychlorobiphenyl on mice. Exp. Mol. Path. 26: 139-160.

Gravis, C.J., R.D. Yates, and I. Chen. 1976. Light and electron microscopic localization of ATPase in normal and degenerating testes of Syrian hamsters. Amer. J. Anat. 147: 419-432.

Gravis, C.J., I. Chen, and R.D. Yates. 1977. Stability of the intra-epithelial component of the blood-testis barriers in epinephrine-induced testicular degeneration in Syrian hamsters. Amer. J. Anat. 148: 19-32.

Gravis, C.J., R.D. Yates, and I. Chen. 1977. Ultrastructure and cytochemistry of epinephrine induced testicular degeneration. **In:** Male Reproductive System: Fine Structure Analysis by Scanning and Transmission Electron Microscopy. R.D. Yates and M. Gordon, eds. Masson Publishing USA Incorporation, New York.

Hansen, J.T. 1977. Morphometric study of the aortic body Type I cell. Experientia 33: 76-78.

Hansen. J.T. 1977. Freeze-fracture study of the carotid body. Amer. J. Anat. 148:295-300.

Herbert, Damon C., Pauline L. Cisneros, and Edward G. Rennels. 1977. Morphological changes in prolactin cells of male rats after testosterone administration. Endocrinology 100:487-495.

Hoage, T.R., and I.L. Cameron 1976. DNA synthesis in the oocyte of the mature mouse: a radioautographic study. Anat. Rec. 186:585-594.

Ishikawa, Hiroshi, Masataka Shiino, Akira Arimura, and Edward G. Rennels. 1977. Functional clones of pituitary cells derived from Rathke's pouch epithelium of fetal rats. Endocrinology, (in press).

Jeter, J.R., Jr., K.M. Knieriem, and I.L. Cameron. 1977. Synthesis of nuclear proteins in mature and immature avian erythrocytes. Cytobios 15: 183-189.

Pool, Thomas B., and J.N. Dent. 1977. The ultrastructure and the hormonal control of product synthesis in the hedonic glands of the red-spotted newt, **Notopthalmus viridescens.** J. Expt. Zool., (in press).

Pool, Thomas B., J.N. Dent, and Kenneth Kemphues. 1977 Neural regulation of product discharge from the hedonic glands of the red-spotted newt, **Notopthalmus viridescens.** J. Expt. Zool., (in press).

Rennels, E.G., D.E. Blask, and J.B. Warchol. 1976. Ultrastructural changes in prolactin cells at rat hemipituitary glands incubated with dopamine. Gunma Symposia on Endocrinology 13: 179-194.

Shiino, Masataka, and Edward G. Rennels. 1976. Electron microscopic observations on depression of pituitary prolactin secretion by vinblastine in the rat. Gunma Symposia on Endocrinology 13: 195-206.

Weaker, Frank J. 1977. The fine structure of the interstitial tissue of the testis of the nine-banded armadillo. Anat. Rec. 187: 11-28.

Yates. R.D., J.A. Mascorro, J.T. Hansen, and I.Chen. 1976. Comparison of the structure of carotid and subclavian bodies and abdominal paraganglia. In: SIF Cells. Fogarty Proceedings #30, DHEW #76-942. O. Eranko, ed., pp. 54-65.

Zimmerman, S., A.M. Zimmerman, I.L. Cameron, and H.L. Laurence. 1977 Δ^1-Tetrahydrocannabinol, cannabidiol and cannabinol on the immune response of mice. Pharmacology, (in press).

News Briefs: Dr. Nancy Smith presented a short course in SEM to the EM staff of the Department of Pathology at The University of Texas Health Science Center at San Antinio.

Dr. Louis Poirier from Laval University in Quebec, Canada, gave a seminar to the Anatomy Department in January entitled "Distribution of acetyl cholinesterase with different structures of the extrapyramidal system following the administration of DFP in the monkey." and in February, Dr. Jack Finerty from Louisiana State University School of Medicine in New Orleans gave a seminar entitled "Parabiosis".

The following members of the Anatomy Department presented and/or co-authored papers at the Annual Meeting of the American Association of Anatomists in Detroit in May 1977: Drs. E. Adrian, E.P. Bowie, D. Blask, A. Burton, I. Cameron, H.C. Dung, C. Gravis, J. Hansen, D. Herbert, M. Houston, H. Ishikawa, W. McNutt, W. Morgan, T. Pool, R.J. Reiter, E.G. Rennels, R. Schelper, P. Sheridan, M Shiino, N. Smith, M. Vaughan, F. Weaker, and V. Williams; L. Johnson, J. McGill, E. Panke, R. Philo, K. Rudeen, R. Sparks, J. Vriend, M. Welsh, and M.G. Williams.

Drs. D.C. Herbert and M.L. Houston were Co-Chairmen of scientific sessions at the Anatomy Meetings in Detroit in May 1977.

TSEM e⁻

CORPORATE MEMBERS

Acromatic Industries, Inc., P.O. Box 12548, Dallas, Texas 75225.

AEI Scientific Apparatus, Inc., Terrance J. Godding, 500 Executive Blvd., Elmsford, New York 10523. (914) 592-4620.

American Optical Corporation, L.B. Read, P.O. Box 1929, Dallas, Texas 75221. (214) 747-8361.

Advanced Metals Research Corporation, Tom Baum, 1910 Hickory Creek, Humble, Texas 77338. (713) 446-3585.

Carl Zeiss, Inc., Rudolph Dietter, Building 2, Suite 191, 3233 Weslayan, Houston, Texas 77027. (713) 629-0730.

Collins Radio Group — Rockwell Instruments, Donald L. Willson, Mail Station 406-146, Richardson, Texas 75080.

Coates & Welter Instrument Corporation, A. Baron Challice, 777 North Pastoria Avenue, Sunnyvale, California 94086. (408) 732-8200.

Cambridge-Imanco, Elio A. Ronchini, Jr., or Steve Miller, 8020 Austin Avenue, Morton Grove, Illinois 60053. (312) 966-1010.

DuPont/Sorvall, Jim Gordon, 91 Talmage Hall Drive, Conroe, Texas 77301. (713) 667-6273 or 273-4809.

Electron Microscopy Sciences, M.J. Oulton, P.O. Box 251, Ft. Washington, Pennsylvania 17034.

Ernest F. Fullam, Inc., Claude J. Arceneaux, Route 2, Box 61, Lafayette, Louisiana 70501. (318) 896-6456.

ETEC Corporation, James W. Rue, 3392 Investment Boulevard, Hayward, California 94545. (415) 783-9210.

George Lange & Company, Mr. George Lange, 6630 South Main Street, Houston, Texas 77025.

H. Dell Foster Co., Richard T. Church, 14703 Jones Maltsberger Road, P.O. Box 32581, San Antonio, Texas.

International Scientific Instruments, Bob Seibert, 6655 Hillcroft, Suite 100, Houston, Texas 77081. (713) 777-0321.

JEOL, USA, Inc., Paul Enos, 412 Shelmar Drive, Euless, Texas 76039. (817) 267-6011.

Kevex, Dick Cushing, 898 Mahler Road, Burlingame, California 94010. (415) 697-6901.

Ladd Research Industries, Inc., Mr. Ted Willmorth, 1209 Dogwood Drive, Kingston, Tennessee 37763. (802) 658-4961.

L.K.B. Instruments, Inc., W. Allan Doty, Jr., 5300 Telephone Road, Houston, Texas. (713) 228-4062.

Logetronics, Daniel P. Short, 7001 Loisdale Road, Springfield, Virginia 22150. (703) 971-1400.

Olympus Corporation, Mr. Don Gordon, P.O. Box 44008, Dallas, Texas 75234. (214) 747-6989.

Ortec, Ron Keller, 4511 Merrie Lane, Bellaire, Texas 77401. (713) 528-5775.

Overall Engineering, Edsel Overall, 15755 Daleport, Dallas, Texas 75248. (214) 233-2311.

Perkin-Elmer Corporation, Mike Mullen, 11110 Los Alamitos Boulevard, Suite 202, Los Alamitos, California 90720. (213) 596-2512.

Philips Electronic Instruments, George Brock, 7302 Harwin Drive, Suite 106, Houston, Texas 77036. (713) 782-4845.

Polaron Instruments, Inc., Dermot Dinan, 1202 Bethlehem Pike Line, Lexington, Pennsylvania 18932. (215) 822-3364/5.

Polysciences, Dr. David B. Halpern, President, Warrington, Pennsylvania 18976.

Princeton Gamma Tech, Dick Neiman, 21718 Rotherham, Spring, Texas 77373. (713) 225-6160.

Schares Instrument Corporation, Mr. Helmut Schares, 12666 Rip Van Winkle, Houston, Texas 77024. (713) 468-4460.

Seimens Corporation, Mr. Dietrich Voss, 11506 South Main, Suite 400, Houston, Texas 77025. (713) 661-3601.

S.P.I. Supplies, Betty Graber, P.O Box 342, West Chester, Pennsylvania 19380. (201) 549-9350.

Technic, Inc., Robert Barr, 5510 Vine Street, Alexandria, Virginia 22310. (703) 971-9200.

Technical Instrument Co., 13612 Midway Road, Suite 333, Dallas, Texas 75240. (214) 387-0606.

Tracor Northern, Mr. Orth, 2551 West Beltline Highway, Middleton, Wisconsin 53562. (608) 836-6511.

Ted Pella, Inc., Thomas P. Turnbull, P.O. Box 510, Tustin, California 92680. (714) 557-9434.

William H. Talley Company, Mr. Bill Talley, P.O. Box 22574, Houston, Texas 77027.

Job Opportunities

Situation Wanted — V. K. Berry, M.S. (Chemistry), Ph.D. (Metallurgy), Expected to complete by May '77. Over 12 years extensive experience in all aspects of electron microscopy both in biological and physical sciences. Experience in TEM, SEM, diffraction and x-ray analysis. Capable to organize, manage and supervise an excellent EM facility. Expertise in all techniques and samples. Publications: Ph.D. dissertation in Biometallurgy. Desires a mature position in research, teaching and/or supervision, organization, directing a quality EM facility in TEM, SEM, or both. Write to: V.K. Berry, Box 2391, Campus Station, Socorro, New Mexico 87801. Residence (505) 835-5279 or Office (505) 835-5229.

Situation Wanted — Barbara Bruton, M.A., Eight and one-half years research experience under Dimitrij Lang doing quantitative electron microscopy of nucleic acids. Prior experience in microbiology especially psychology and food industry quality control. Seeking position requiring initiative, responsibility for a smooth running laboratory, and involvement in research projects. Current address: University of Texas at Dallas, Biology Programs, Mail Station FO 3.1, P.O. Box 688, Richardson, Texas 75080.

Position Available — Electron Microscopy Technician, B.S. preferrable in biology or chemistry with training in TEM and/or SEM. Contact Ronald F. Dodson, Ph.D., Chief, Division of Experimental Pathology, P.O. Box 2003, East Texas Chest Hospital, Tyler, Texas 75710.

Comparative Pathologist, M.D. or D.V.M. with Ph.D. Pathology Board or ACVP eligiblity or certification desirable. Experience in rodent pathology, careinogenesis, clinic pathology, immunology, histochemistry, autoradiography, or electron microscopy helpful. Duties include (1) involvement in multidisciplinary projects with some individual research time available, (2) participation in histopathologic examination of tissues from rodents involved in carcinogenic, mutagenic and teratogenic studies, (3) teaching, (4) involvement in graduate and under graduate education, (5) involvement in interdisciplinary graduate toxicology program. Excellent clinical pathology and electron microscopy support. Salary commensurate with qualification/experience. Send resume to: Project Director, RSP, National Center for Toxicological Research, Jefferson, AR 72079. Equal Opportunity Employer.

Position Available — An opportunity to provide EM technical services for the basic science departments of a medical school. TEM and SEM experience required, background with diverse specimens (eg. bacteria, embryos, cell fractions) and techniques (eg. autoradiography, cytochemistry, EDX) helpful. Available within next three months. For more information, contact: Robert W. Rice, PhD, Program in Medicine, Teague Research Center, Texas A&M University, College Station, TX 77843.

Electron Microscopy Manager — Opening for individual providing technical assistance, maintenance of equipment, laboratory management and some instruction in electron microscopy. One year of previous EM employment experience and working knowledge of both TEM and SEM and related techniques required. Excellent opportunity for industrious individual technically proficient with both biological and physical science background. BS degree required, advanced degree preferred. Submit resume, transcript, and three letters of reference to: Dr. Richard E. Crang, Dept. of Biological Sciences, Bowling Green State University, Bowling Green, OH 43403. An equal opportunity/affirmative action employer.

Situation Wanted — Raul Joseph Alvarado, 5300 Tropicana, El Paso, TX 79924. (915) 751-0691. Single, 5-10, 180 lbs, born July 24, 1951. Wants career in medical field as a Laboratory Technician. Majored in Microbiology at El Paso Community College, GPA 3.6 on a 4.0 scale. Presently employed as Bio-Lab aide, electron microscopy, Dept. of Pathology, William Beaumont Army Medical Center, El PASO, TX. Has been recommended by Bernhard E.F. Reimann, Dr., rer. nat., Chief, at William Beaumont Army Medical Center. Dr. Reimann is in the process of training Mr. Alvarado and will be available for full-time job on Jan. 21, 1977. Other references and a complete resume are available.

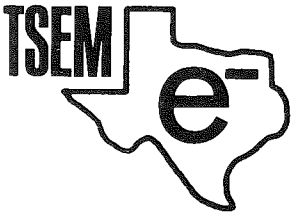

REGIONAL EDITORS

Ronald F. Dodson, Department of Neurology and Pathology, Baylor College of Medicine, Texas Medical Center, Houston, Texas 77025. (713) 790-4753.

Joanne T. Ellzey, Biological Sciences, The University of Texas at El Paso, El Paso, Texas 79968. (915) 749-5609.

D. C. Herbert, Department of Anatomy, The University of Texas Health Science Center at San Antonio, San Antonio, Texas 78284. (512) 696-6537.

James K. Butler, Department of Biology, The University of Texas at Arlington, Arlington, Texas 76010. (817) 273-2871.

Ron Gruener, The University of Texas Medical School at Houston, Neurobiology and Anatomy, 6400 West Cullen Boulevard, Houston, Texas 77025. (713) 792-4885.

Bernell Dalley, Department of Anatomy, Texas Tech University School of Medicine, Lubbock, Texas 79409. (806) 742-5277.

Marilyn Smith, Department of Biology, Texas Women's University, Denton, Texas 76204.

Jo Ann Shively, Department of Veterinary Anatomy, Texas A&M University, College Station, Texas 77843. (713) 845-2828.

Joe A. Mascorro, Department of Anatomy, Tulane School of Medicine, New Orleans, Louisiana 70112. (504) 588-5255.

Ruben Ramirez-Mitchell, Cell Research Institute, Biology Lab 311, The University of Texas, Austin, Texas 78709. (512) 471-3965.

Mary Tobelman, Department of Cell Biology, The University of Texas Southwestern Medical School, Dallas, Texas 75235. (214) 631-3220.

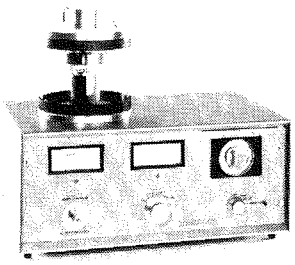

"Cool" Sputtering for S.E.M.

Having pioneered the use of diode sputtering for SEM sample coating. Polaron has now gone a step further. The Series II unit has been designed to completely eliminate specimen heating while coating. This has been achieved by the design of a novel target arrangement incorporating magnetic fields thus eliminating specimen heating by electron bombarbment as found in conventional systems. Another "first" from Polaron.

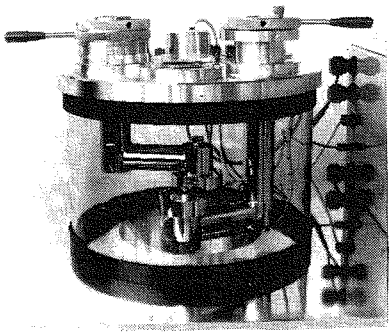

Freeze Etching

If you have at some time considered the use of the freeze etching technique in your laboratory but have been dismayed by the cost and complexity of the apparatus offered then this new system from Polaron will make you reconsider. Our module sells at half the price of its nearest competitor and processes more work in a day than any other can achieve in a week. Call us and we'll tell you how we do it.

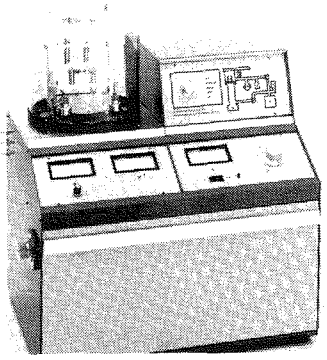

Automatic Coaters for TEM

If you want to buy a large floor standing high vacuum evaporator with facilities for freeze etching or ion etching we'll sell you one. But we think you probably only need our new bench top evaporator:—

- ☐ 10" belljar with carbon and metal evaporation jigs
- ☐ automatic pump down cycle
- ☐ 3" diff pump and two stage rotary
- ☐ half the price of a big system

The three instruments listed above are just a few from our large range of products designed for the electron microscopist. Among the other instruments available are, briefly, Critical Point Apparatus, Electron Micrograph Optical Diffractometer, Electropolishing Units, Ion-Beam Thinning Device, Water-coolers and a complete range of Vacuum Evaporators.

Our general accessories catalogue carries a complete range of everyday consumables required by the E.M. Laboratory.

For further information, or a demonstration of our equipment please do not hesitate to call us at the address below.

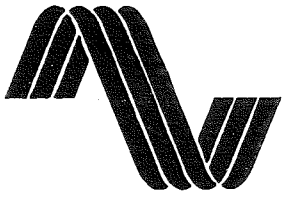

POLARON INSTRUMENTS INC.
1202 BETHLEHEM PIKE
LINE LEXINGTON, PA. 18932
215: 822-3364/5

SIEMENS

The all new

ELMISKOP ST 100 F

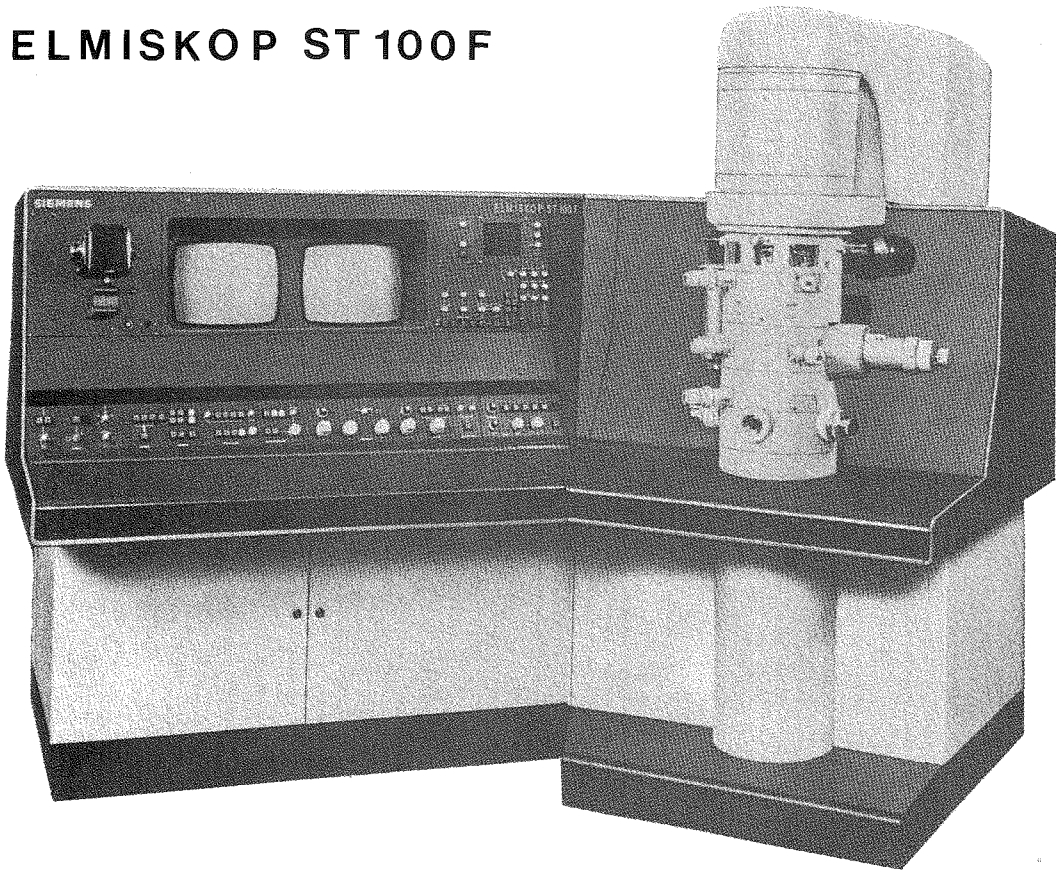

Scanning Transmission Electron Microscope

- Field Emission Gun
- 10 KV—100 KV
- 2 AU Resolution
- Fully eucentric Stage
- Ion Getter Pumps
- Energy Loss Analyzer

SIEMENS Corporation · 11506 South Main Street ·
Houston · Texas 77025 · (713) 661-3601 ·

From Hitachi/Perkin-Elmer a powerful TEM lineup

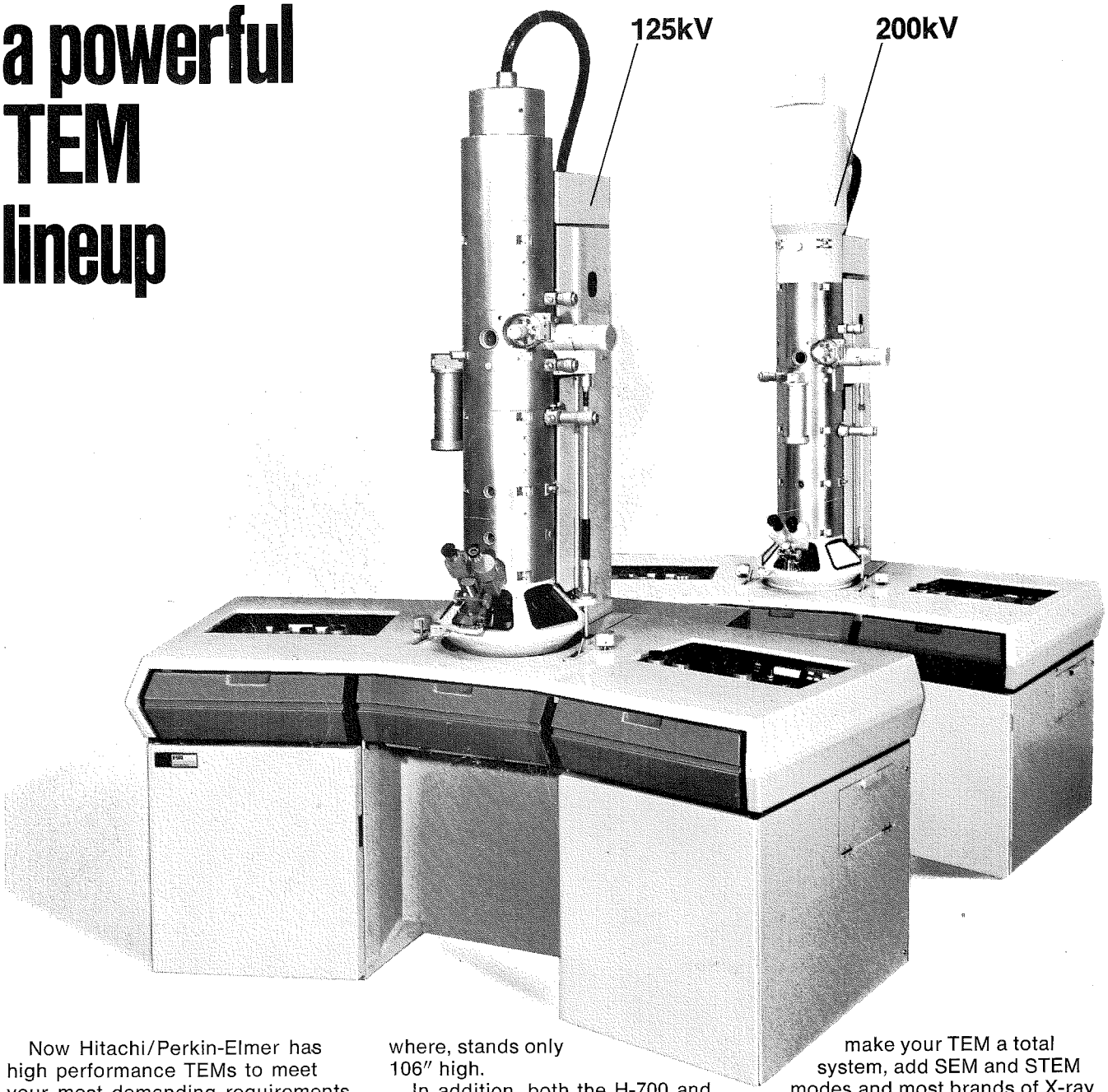

Now Hitachi/Perkin-Elmer has high performance TEMs to meet your most demanding requirements.

First, there's the H-500: 10-125 kV accelerating voltages, 100X to 800,000X magnification and a guaranteed resolution of 1.4Å.

If you want even more, choose the H-700: accelerating voltages from 75 to 200 kV, a resolution of 2.8Å and magnification from 200X to 300,000X. The H-700 fits most anywhere, stands only 106″ high.

In addition, both the H-700 and the H-500 have our patented zoom feature: just turn one knob to change magnification, without losing focus. They also have an objective lens yoke that accepts either top or side entry specimen stages.

Automatic control of routine functions is another plus, includes fully automatic camera and evacuation systems. What's more, you can make your TEM a total system, add SEM and STEM modes and most brands of X-ray analysis equipment at any time.

So, if you want high performance in a TEM, choose from the Hitachi/Perkin-Elmer lineup. For details and/or a demonstration, call or write. Perkin-Elmer, Instrument Marketing Division, 411 Clyde Avenue, Mountain View, CA 94043 Phone: (415) 961-0461.

PERKIN-ELMER